ASC Coordinates: Rev 4.3

SDS-2.0

Jonathan McDowell

1998 Aug 4

Contents

I Part 1: Mission-independent formulation **6**

1 General Introduction **6**
1.1 Update notes . . . 6
1.2 Notational conventions . . . 6
1.2.1 Pixel convention . . . 6
1.2.2 Vector and coordinate notation . . . 6
1.2.3 Rotation and translation of Cartesian systems . . . 7
1.2.4 Spherical polar coordinates . . . 8

2 Data Analysis Coordinate Systems - Imaging **8**
2.1 General model of the system . . . 8
2.2 Data Analysis 1: Telemetry to Tangent Plane . . . 9
2.2.1 Telemetry to Chip coordinates . . . 9
2.2.2 Tiled Detector Coordinates . . . 10
2.2.3 Local Science Instrument coordinates . . . 11
2.2.4 Mirror coordinates . . . 14
2.2.5 Pixel planes for intermediate systems . . . 19
2.3 Data Analysis 2: Tangent Plane to Sky . . . 19
2.3.1 Sky Pixel Coordinates . . . 19
2.3.2 Physical Tangent Plane coordinates . . . 19
2.3.3 Physical Sky Plane coordinates . . . 20
2.3.4 J2000 Celestial Coordinates . . . 20
2.4 Simulation: Sky to Telemetry . . . 21

2.4.1 Mirror Spherical Coordinates to Focal Surface Coordinates . . . 21
2.4.2 Focal Surface or Mirror Nodal Coordinates to CPC coordinates . . . 21
2.4.3 Chip coordinates . . . 23
2.5 Summary of coordinate systems . . . 23

3 Data Analysis Coordinate Systems - Gratings **24**
3.1 Data Analysis: Grating data . . . 24
3.1.1 Grating Zero Order Coordinates (GZO-1.0) . . . 24
3.1.2 Grating Angular Coordinates (GAC-1.0) . . . 25
3.1.3 Grating Diffraction Coordinates (GDC-1.0) . . . 26
3.1.4 Grating Diffraction Plane Pixel Coordinates (GDP-1.1) . . . 26
3.1.5 Dispersion relation . . . 26

II Part 2: AXAF systems **27**

4 ACIS **27**
4.1 Instrumental details . . . 27
4.1.1 ACIS readout coordinates . . . 27
4.1.2 ACIS Fast Window mode . . . 28
4.2 2-D detector coordinates: TDET parameters . . . 29
4.3 3-D chip locations: CPC to LSI transformation parameters . . . 30

5 HRC **32**
5.1 Overview . . . 32
5.1.1 3-D chip locations: CPC to LSI parameters . . . 32
5.1.2 2-D detector coordinates: TDET parameters . . . 33
5.2 Instrumental details . . . 34
5.2.1 HRC physical layout and Tap Coordinates (HRC-6.0) . . . 34
5.2.2 Deriving linear tap coordinates from HRC telemetry . . . 34
5.2.3 HRC Chip Coordinates (HRC-1.1) . . . 36

6 The SIM **42**
6.1 Chip orientation summary tables . . . 42
6.2 Relative positions of instruments . . . 42
6.3 Aimpoints . . . 43

7 The HRMA (flight) **43**
7.1 HRMA nodal coordinates . . . 43
7.2 Focal and Tangent plane systems . . . 43
7.2.1 Mosaicing XRCF images . . . 45

7.3 Angular systems . . . 45
7.3.1 HRMA Left Handed Spherical Coordinates (AXAF-HSC-1.1) . . . 45
7.3.2 HRMA Right Handed Spherical Coordinates (AXAF-HSC-1.2) . . . 46
7.3.3 HRMA rotation coordinates (Pitch and Yaw) (AXAF-HSC-3.0) . . . 46
7.3.4 HRMA Source coordinates (AXAF-HSC-2.1) . . . 47

8 HETG and LETG **47**

9 XRCF **49**
9.1 XRCF coordinates . . . 49

10 ACIS-2C **49**

11 HSI **51**
11.1 Instrument origins . . . 52
11.2 HRMA motion . . . 52
11.2.1 XRCF to MNC transformation . . . 53
11.3 HXDS Motion . . . 54
11.4 FAM Motion . . . 54
11.5 FAM Motion, old copy . . . 55

12 AXAF Spacecraft **56**
12.1 Project coordinate systems . . . 56
12.1.1 Spacecraft coordinates (SC-1.0) . . . 56
12.1.2 HRMA coordinates (HRMA-2.0) . . . 57
12.2 Project Coordinate Systems . . . 59
12.2.1 Orbiter coordinate system . . . 59
12.2.2 Payload coordinate system . . . 59
12.2.3 The Telescope Ensemble Coordinate System . . . 60
12.2.4 Optical Bench Assembly system . . . 60
12.2.5 OTG Coordinates (OTG-2.0) . . . 60
12.2.6 Project FPSI Coordinate System . . . 60
12.2.7 SIM and ISIM coordinates . . . 60
12.2.8 SAOSAC coordinates (HRMA-3.0) . . . 61
12.2.9 Summary of useful HRMA Cartesian systems . . . 61

List of Tables

1 Default axis orientations . . . 16
4 Tiled Detector Plane systems . . . 29

5 Parameters of Tiled Detector Coordinate definitions 29
6 ACIS Chip corner locations in ACIS-I LSI coordinates 31
8 HRC chip (i.e. grid) corner locations in LSI coordinates 32
9 Tiled Detector Plane systems 33
10 Parameters of Tiled Detector Coordinate definitions 33
11 HRC-S1 TELV, v and CHIPY 36
12 HRC electronically meaningful coordinate ranges 37
13 HRC-S boundaries (Revised May 98) 38
14 HRC-I boundaries 40
15 Euler angles in degrees for CPC to LSI coordinates 42
16 Location of instrument origin on Translation Table 42
17 SIM position offsets for nominal focus positions 43
20 GDC pixel image centers 48
21 GDP Pixel Sizes (assuming flight Rowland radius) 48
22 Grating properties 49
23 Tiled Detector Plane systems - ACIS-2C 49
24 Parameters of Tiled Detector Coordinate definitions 50
25 ACIS-2C chip corner locations in ACIS-2C LSI coordinates 51
26 HSI boundaries 51
27 Parameters of Tiled Detector Coordinate definitions 51
28 HSI chip corner locations in HSI LSI coordinates 52
29 Location of instrument origin on Translation Table, XRCF 52
30 Assumed Misalignments 55
31 Interesting points in spacecraft and HRMA nodal coordinates 57
32 Geometrical layout of mirrors and detectors: Value of MNC X Coord X_N 58
33 Mirror radii, mm 58

List of Figures

1 Pixel convention. 7
2 The relationship between CHIP and Tiled Detector coordinates. 10
3 The relationship between CHIP, LSI and STT coordinates. 12
4 The instrument compartment (dashed line) may be misaligned with the telescope mirrors. At calibration, this misalignment (highly exaggerated here) may be significant and variable as the mirror is tilted with respect to the instruments. The instrument bench moves with respect to the instrument compartment, as indicated by the arrow. 13
5 The relationship between STT and STF coordinates. 13

6 The Tangent Plane Coordinate system describes the incoming rays, while the Focal Plane Coordinates system describes the angular position of rays emerging from the mirrors. The rays then intersect one of several inclined detector planes, causing events whose locations are described in tiled detector coordinates. 15
7 The different pixel plane coordinate systems. Distorting effects are highly exaggerated. 17
8 Imaging the sky in LSI coordinates 18
9 Coordinate systems used in data analysis, 1: Imaging data analysis. 21
10 Coordinate systems used in data analysis, 2: Grating data analysis. 22
11 Grating Zero Order coordinates 25
12 Grating Diffraction coordinates 26
13 ACIS readout nodes 29
14 Relationship of HRC-S pixels to the physical instrument. 38
15 HRC-I pixel axes. 40
16 The AXAF SIM Translation Table, showing the flight focal plane instruments to scale. Distances are in mm. Coordinate system is AXAF-STT-1.0. 62
17 HRMA Nodal and STF Coordinates showing the on-orbit configuration. 63
18 HRMA spherical coordinates 63
19 HRMA source coordinates 63
20 XRCF Coordinates showing the general configuration with HRMA, DFC and LSI coordinate systems 64
21 XRCF Coordinates showing the general configuration with HRMA and LSI coordinate systems 64
22 Schematic of interesting points in the spacecraft 65

Part I
Part 1: Mission-independent formulation

1 General Introduction

There are a lot of different coordinate systems used in the AXAF program, mostly intended for use in constructing and aligning the hardware. This memo is intended to give the ASC SDS group's current understanding of the relationships between them (mirror metrology systems are not yet included) and to define many more systems, which are useful for data analysis of observations both in flight and at XRCF.

1.1 Update notes

Minor update to XRCF focal plane systems FP-4.1, FP-3.1 (1997 Feb 27); General update post XRCF, especially to HRC values (1997 Dec 21). Corrected HRC TDET system (1998 May 12).

1.2 Notational conventions

Each of the pixel coordinate systems is identified by a label beginning with the string ASC, followed by a string identifying the system, and ending with a version number. For example, ASC-CHIP-1.0 (loosely, CHIP coordinates) refers to a pixel system defined by the equation immediately following its bold-face first mention, and satisfying the pixel convention discussed below.

1.2.1 Pixel convention

In all cases where we use discrete **pixel numbers**, the corresponding real-valued, continuous **pixel coordinates** are defined to be equal to the pixel number at the center of the pixel. We further recommend that for finite detector planes, one corner be designated as the lower left corner, LL. Then the pixel which has LL as one of its corners (i.e. the lower left pixel) shall be numbered (1,1) so that its center has coordinates (1.0, 1.0). The coordinates of the LL point itself are (0.5, 0.5). If the detector is rectangular with sides of length XMAX, YMAX the pixel coordinates then run from (0.5, 0.5) in the lower left corner (LL) to (XMAX+0.5, YMAX+0.5) in the upper right corner (UR) while the pixel numbers in each axis run from 1 to XMAX, 1 to YMAX.

1.2.2 Vector and coordinate notation

A bold face symbol e.g. $\boldsymbol{B}$ denotes a point in 3D space. The notation $Y_A(\boldsymbol{B})$ denotes the Y coordinate of point $\boldsymbol{B}$ in the 3-dimensional Cartesian coordinate system A. When we refer to a point as an argument in this way we usually get lazy and omit the boldface, e.g. $Y_A(B)$. The

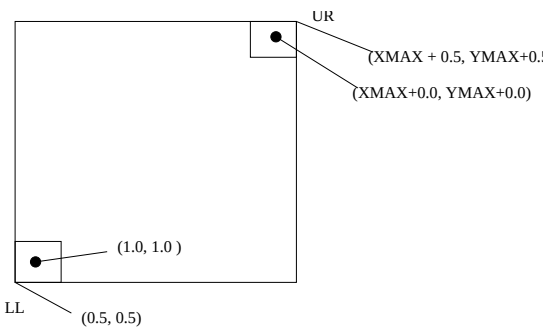

Figure 1: Pixel convention.

notation $P_A(B)$ denotes the triple $(X_A(B), Y_A(B), Z_A(B))$, i.e. the coordinates of $\boldsymbol{B}$ in the A coordinate system. (P is not in boldface since it is not a vector - it is in a specific coordinate system.)

1.2.3 Rotation and translation of Cartesian systems

We define an Euler rotation $\mathrm{Rot}(\phi_E, \theta_E, \psi_E)$ of a Cartesian system X,Y,Z to be the product of three rotations

$$\mathrm{Rot}(\phi_E, \theta_E, \psi_E) = \mathrm{Rot}_1(Z, \psi_E)\mathrm{Rot}_1(Y, \theta_E)\mathrm{Rot}_1(Z, \phi_E) \tag{1}$$

where the rotations apply to the successively rotated axes from right to left in the usual sense of matrix multiplication,

The general transformation from a cartesian system A to a system B involves a scaling, a translation, and a rotation. This may be described by seven numbers: the scale factor K_{AB} (choice of units), the position vector $P_B(A0) = (X_B(A0), Y_B(A0), Z_B(A0))$ of the origin of A in the B system, and the three Euler angles ϕ_E, θ_E, ψ_E of the rotation R(A,B) from A to B,

$$\begin{aligned} R(A,B) &= Rot(\phi_E, \theta_E, \psi_E) \\ &= \begin{pmatrix} \cos\phi_E \cos\theta_E \cos\psi_E - \sin\phi_E \sin\psi_E & \sin\phi_E \cos\theta_E \cos\psi_E + \cos\phi_E \sin\psi_E & -\sin\theta_E \cos\psi_E \\ -\cos\phi_E \cos\theta_E \sin\psi_E - \sin\phi_E \cos\psi_E & -\sin\phi_E \cos\theta_E \sin\psi_E + \cos\phi_E \cos\psi_E & \sin\theta_E \sin\psi_E \\ \cos\phi_E \sin\theta_E & \sin\phi_E \sin\theta_E & \cos\theta_E \end{pmatrix} \end{aligned} \tag{2}$$

Then coordinates of a general point G

$$P_A(G) = (X_A(G), Y_A(G), Z_A(G)) \tag{3}$$

may be converted to

$$P_B(G) = (X_B(G), Y_B(G), Z_B(G)) \tag{4}$$

using the formula

$$\boxed{P_B(G) = R(A,B)K_{AB}P_A(G) + P_B(A0)} \tag{5}$$

If

$$R(A,B) = Rot(\phi_E, \theta_E, \psi_E) \tag{6}$$

then

$$R(B,A) = Rot(\pi - \psi_E, \theta_E, \pi - \phi_E). \tag{7}$$

Further, if C is related to B by reflection about the X axis, i.e. $Y_C = -Y_B, Z_C = -Z_B$ then

$$R(A,C) = Rot(\phi_E, \pi + \theta_E, \pi - \psi_E). \tag{8}$$

1.2.4 Spherical polar coordinates

We also use spherical polar coordinate systems. The WCS paradigm describes general rotations of a spherical polar coordinate system. We define the native cartesian axes X,Y,Z of a spherical polar system (r, θ, ϕ) by the equation

$$(X, Y, Z) = r\mathcal{S}(\theta, \phi) = (r\cos\phi\sin\theta, r\sin\phi\sin\theta, r\cos\theta) \tag{9}$$

so that the north pole is through the positive Z axis and the azimuth is zero along the positive X axis and 90 degrees along the positive Y axis. Any other choice of spherical coordinates (r, θ', ϕ') may be defined by specifying the Euler rotation matrix which rotates the corresponding native systems into each other.

In the appendix I derive

$$\boxed{\begin{array}{rcl} \theta' & = & \cos^{-1}\left(\cos\theta_E\cos\theta + \sin\theta_E\sin\theta\cos(\phi - \phi_E)\right) \\ \\ \phi' & = & \arg\left(\cos\theta_E\sin\theta\cos(\phi-\phi_E) - \sin\theta_E\cos\theta, \sin\theta\sin(\phi-\phi_E)\right) - \psi_E \end{array}} \tag{10}$$

2 Data Analysis Coordinate Systems - Imaging

2.1 General model of the system

We model an observatory consisting of several telescopes. Each telescope has an optical system (loosely, 'mirror') which images the sky by converting incoming photon paths to outgoing photon paths in a well determined way, and an instrument compartment. In the instrument compartment is an instrument table on which are mounted several instruments. The instruments are fixed with respect to the instrument table, but the table may move relative to the instrument compartment. Further, the instrument compartment itself may move relative to the optical system (for AXAF, this happens only at calibration). Each instrument consists of one or more fixed 'chips' or planar detector surfaces of finite area. For AXAF, these chips are all rectangular, although note that the ROSAT PSPC is circular. Finally, each chip is subdivided into rectangular (usually square) 'detector pixels', enumerating the set of distinct locations that can be represented in the instrument telemetry

stream. (In the case of CCDs, these correspond to physical CCD pixels, while in microchannel plate detectors they are arbitrarily set by the electronics).

The information available to us, the telemetry position, is two dimensional, but to infer the final two dimensional angular incoming sky direction we must calculate a photon position in three dimensional space. Every time we want to make an image, we use a two dimensional pixel plane (possibly losing information in a third dimension). So the three types of coordinate system we will use are:

- Two dimensional pixel plane
- Two dimensional spherical angular coordinates
- Three dimensional cartesian coordinates.

2.2 Data Analysis 1: Telemetry to Tangent Plane

2.2.1 Telemetry to Chip coordinates

The telemetry coordinates of a photon are a collection (n-tuple) of integers. The formats may be very different from instrument to instrument; for instance, the HRC telemetry coordinates consist of two Tap values and six voltages, while the ACIS telemetry coordinates are directly given as pixel numbers. For each instrument, we provide a rule to convert from telemetry coordinates to our standard data analysis **chip pixel coordinates** which run from 1 to XMAX, 1 to YMAX. They define a logical plane extending from coordinate 0.5 to XMAX+0.5, 0.5 to YMAX+0.5. In other words, the center of pixel number (1,1) is (1.0, 1.0), and its lower left corner is (0.5, 0.5). The logical plane may be larger than the actual set of possibly active pixels. For instance, for a circular detector such as the ROSAT PSPC, we extend this logical chip pixel coordinate plane to be rectangular. This chip pixel coordinate system is labelled as ASC-CHIP-1.0.

The corresponding physical coordinate system is a three dimensional Cartesian system called **Chip Physical Coordinates (CPC)**, giving the physical location of a detected photon event on the active area surface. They are fully defined in terms of the chip pixel coordinates when the pixel size Δ_p and the array size XMAX x YMAX is given.

$(X_{CPC}, Y_{CPC}, Z_{CPC})$ are defined to have units of mm. The CPC X and Y axes are coincident with the chip X and Y axes, and the Z axis completes a right handed set. The CPC Z coordinate of any point in the chip has a value of 0.0. The X and Y coordinates run from 0.0 to XLEN and YLEN, where $XLEN = XMAX * \Delta_p$ and $YLEN = YMAX * \Delta_p$.

Thus if a photon lands at Chip Physical Coordinates X_{CPC}, Y_{CPC} its chip pixel coordinates **(ASC-CHIP-1.0)** are

$$\begin{aligned} CHIPX &= X_{CPC}/\Delta_p + 0.5 \\ CHIPY &= Y_{CPC}/\Delta_p + 0.5 \end{aligned} \tag{11}$$

or

$$\begin{aligned} X_{CPC} &= (CHIPX - 0.5)\Delta_p \\ Y_{CPC} &= (CHIPY - 0.5)\Delta_p \end{aligned} \tag{12}$$

Note that CHIPX and CHIPY are by definition linear, by which I mean that the mapping to real physical space is linear. Now for ACIS it so happens that the true CCD pixels satisfy this condition sufficiently accurately, but for HRC the readout values may require linearization. For HRC and similar instruments, there are actually two kinds of chip pixel coordinate: the RAW chip coordinates do not include a linearization correction, while the standard CHIP coordinates do.

2.2.2 Tiled Detector Coordinates

In an instrument with multiple detector planes, the planes may be tilted with respect to each other, or may be separated by a non-integral number of detector pixels, or both (as in ACIS-I). Projecting onto a 2-D plane (e.g. FP coords) will then lose the identity of individual pixels since one true detector pixel will map to a variable number of square pixels on the projected plane. For recording calibration information like bad pixel lists, it is useful to have a single coordinate system covering the whole instrument which retains true detector pixel identity at the expense of relative positional accuracy. For this purpose we introduced the tiled detector coordinate systems (TDET).

$$\begin{pmatrix} TDETX \\ TDETY \end{pmatrix} = \Delta_i \begin{pmatrix} 1 & 0 \\ 0 & H_i \end{pmatrix} \begin{pmatrix} \cos\theta_i & \sin\theta_i \\ -\sin\theta_i & \cos\theta_i \end{pmatrix} \begin{pmatrix} CHIPX - 0.5 \\ CHIPY - 0.5 \end{pmatrix} + \begin{pmatrix} X0_i + 0.5 \\ Y0_i + 0.5 \end{pmatrix} \tag{13}$$

where the values of H_i, Δ_i and θ_i are different for each chip. H_i gives the handedness of the planar rotation and has values $+1$ or -1, Δ_i gives the sub-pixel resolution factor, and θ_i gives the rotation angle of the chip axes with respect to the detector coordinate axes.

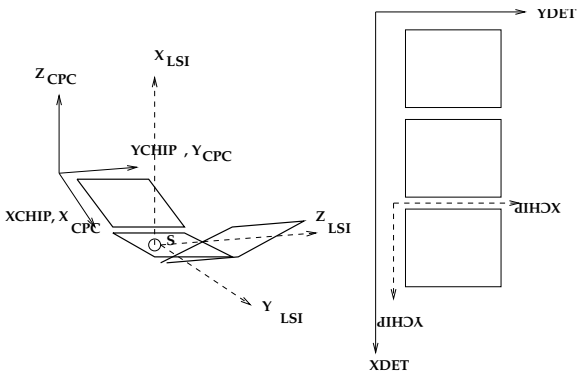

Figure 2: The relationship between CHIP and Tiled Detector coordinates.

2.2.3 Local Science Instrument coordinates

Each instrument has an Instrument Origin which is the nominal focal point for the instrument. For telescopes with movable instrument tables, the actual focal point for a particular observation may be different.

To describe the motion of the instrument table, we use three aligned Cartesian coordinate systems.

- The Science Instrument Translation Frame (STF) coordinate system is fixed in the instrument compartment, and is used to describe the changing position of the instrument table. Its origin is at the flight focus and its axes have +X running from the focus toward the telescope aperture, and +Y and +Z forming a right handed set whose orientation matches that of the observatory coordinates. For AXAF, the direction of instrument table motion is along Z.

- The Science Instrument Translation Table (STT) coordinate system is fixed in the moving instrument table, and is used to describe the positions of the instrument origins relative to each other. The position of its origin is mission-dependent, but the axes are parallel to the STF axes.

- The Local Science Instrument (LSI) coordinate system for each instrument is fixed in that instrument, and is identical to the STT frame but with the origin shifted to the instrument origin.

When the instrument table is moved to put the instrument at its nominal focus position, that means that the LSI origin is coincident with the STF origin. Since the axes are also parallel, STF and LSI coordinates become identical. The STF system therefore measures how much the instrument is offset from its nominal focus.

The STF, LSI and STT coordinate systems are defined to use units of mm. To convert from the LSI system to the STT system, one needs to know the STT coordinates of each LSI origin (i.e. the location of each instrument on the instrument table). To convert to the STF system, one needs to know the instantaneous position of the instrument table, which we describe by giving the STF coordinates of the STT origin O_{STT}.

To convert from a position P(LSI) in LSI coords to P(STF) in STF coords, one then performs the vector sum:

$$P(STF) = P(LSI) + O_{LSI}(STT) + O_{STT}(STF) \tag{14}$$

adding the STT coordinates of the LSI origin and the STF coordinates of the STT origin. When the instrument is at its nominal focus, these two vectors are equal and opposite.

To convert from CPC coordinates to LSI coordinates, we need to carry out a rotation and translation. Each instrument has one LSI coordinate system, and several chips each with its own CPC system. The information we need for each chip to define the transformation is the LSI coordinates of each of the four corners of the chip plane (actually, only three of the four are required).

A general point on the plane is

$$\boldsymbol{r} = \boldsymbol{p_0} + X_{CPC}\boldsymbol{e}_X + Y_{CPC}\boldsymbol{e}_Y \tag{15}$$

where $\boldsymbol{p_0}$ is the origin of CPC coordinates, and $\boldsymbol{e}_X$ and $\boldsymbol{e}_Y$ are the unit vectors along the CPC axes, with $\boldsymbol{e}_Z$ as the unit normal to the plane.

Let us denote the position vectors of the four chip corners as $\boldsymbol{LL}$,$\boldsymbol{UL}$,$\boldsymbol{UR}$,$\boldsymbol{LR}$. Then the unit vectors of the CPC origin and axes in LSI coordinates are

$$\boldsymbol{p_0} = \boldsymbol{LL}, \boldsymbol{e}_X = \boldsymbol{LR} - \boldsymbol{LL}, \boldsymbol{e}_Y = \boldsymbol{UL} - \boldsymbol{LL} \tag{16}$$

and

$$\boldsymbol{e}_Z = \boldsymbol{e}_X \wedge \boldsymbol{e}_Y. \tag{17}$$

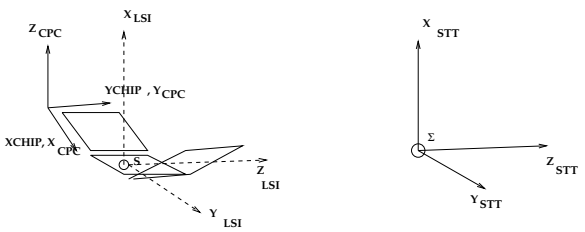

Figure 3: The relationship between CHIP, LSI and STT coordinates.

We can recast this in a rotational formulation,

$$P_G(LSI) = P_{LL}(LSI) + R(CPC, LSI)P_G(CPC) \tag{18}$$

where the matrix is

$$R(CPC, LSI) = \begin{pmatrix} (\boldsymbol{e_X})_X & (\boldsymbol{e_Y})_X & (\boldsymbol{e_Z})_X \\ (\boldsymbol{e_X})_Y & (\boldsymbol{e_Y})_Y & (\boldsymbol{e_Z})_Y \\ (\boldsymbol{e_X})_Z & (\boldsymbol{e_Y})_Z & (\boldsymbol{e_Z})_Z \end{pmatrix} \tag{19}$$

These unit axis vectors can easily be derived from the corner coordinates.

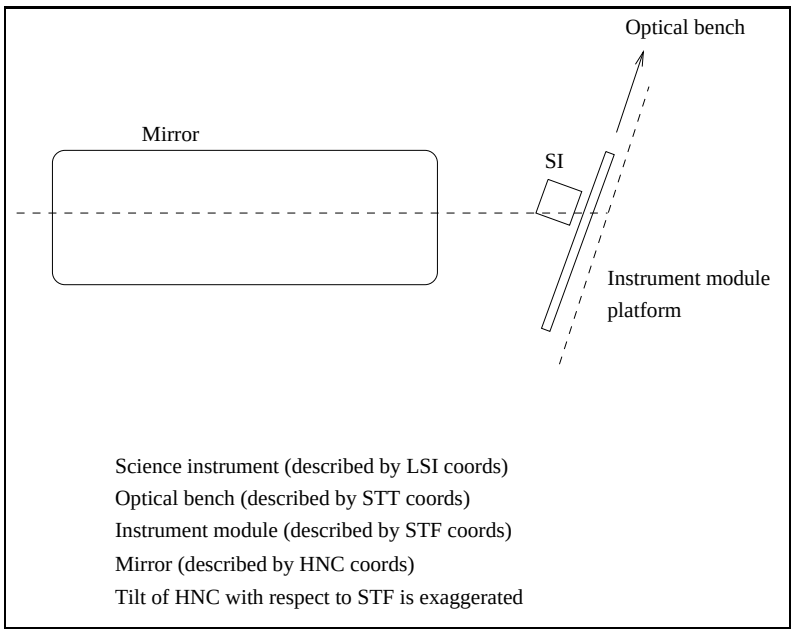

Figure 4: The instrument compartment (dashed line) may be misaligned with the telescope mirrors. At calibration, this misalignment (highly exaggerated here) may be significant and variable as the mirror is tilted with respect to the instruments. The instrument bench moves with respect to the instrument compartment, as indicated by the arrow.

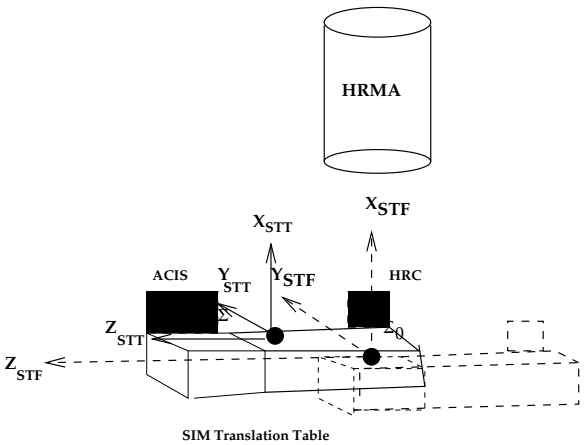

Figure 5: The relationship between STT and STF coordinates, AXAF example. The instrument (SIM) table has moved so that HRC is at the focus.

2.2.4 Mirror coordinates

We now specialize to a simple optical system which can be modelled to first order as a thin lens with an optical node N from which rays appear to emerge toward a detector. This simple description is fine for the AXAF HRMA, but won't apply directly to the complicated optical path of the AXAF Aspect Camera. The origin of mirror coordinates (labelled here as MNC for Mirror Nodal Coordinates, in previous versions of the document HNC for HRMA Nodal Coordinates) is the nominal optical node of the mirrors. The +X axis goes from the node toward the entrance aperture, and the Y and Z axes complete a right handed system. To first order, an incoming ray with MNC direction cosines $(-X_N, Y_N, Z_N)$ emerges from the mirror with direction cosines $(-X_N, -Y_N, -Z_N)$. (We use the subscript 'N' for mirror nodal coordinates).

The mirror has a nominal focal length f, and a nominal focus at mirror coordinates (-f, 0, 0). We define Focus Coordinates (FC-1.0) as a cartesian system identical to MNC coordinates but with its origin at the focus. Thus

$$P(MNC) = (-f, 0, 0) + P(FC) \tag{20}$$

The nominal connection between FC and STF coordinates is

$$P(FC) = P(STF) \tag{21}$$

However, we support the more general alignment

$$P(FC) = O_{STF}(FC) + R(STF, FC)P(STF). \tag{22}$$

This equation allows us to handle the inversion of the HRMA with respect to the instrument compartment that was originally planned for XRCF.

Associated with the MNC system are two spherical coordinate systems. Mirror Spherical Coordinates measure the off axis angle and azimuth of an incoming ray, and their pole is the MNC $+X_N$ axis. Focal Surface Coordinates measure the off axis angle and azimuth of an emerging ray, with pole at the $-X_N$ axis (toward the focus). Each of these spherical coordinate systems has an associated family of pixel plane coordinate systems (parameterized by the selected pixel size), tangent to the pole of the sphere.

The generic Focal Plane Pixel coordinates are

$$\begin{aligned} FPX &= FPX0 + t_x \Delta_s^{-1}(Y_N/|X_N|) \\ FPY &= FPY0 + t_y \Delta_s^{-1}(Z_N/|X_N|) \end{aligned} \tag{23}$$

where t_x, t_y are sign parameters which control the orientation of the image. Δ_s is the pixel size in radians. The actual physical pixel size at the focus, for focal length f, is

$$\Delta_p = f\Delta_s \tag{24}$$

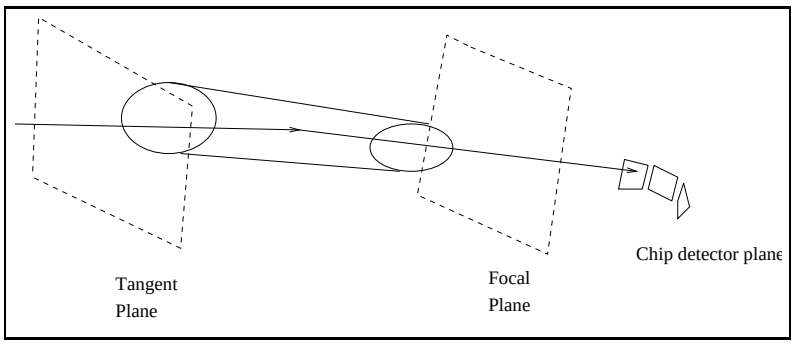

Figure 6: The Tangent Plane Coordinate system describes the incoming rays, while the Focal Plane Coordinates system describes the angular position of rays emerging from the mirrors. The rays then intersect one of several inclined detector planes, causing events whose locations are described in tiled detector coordinates.

A focal plane pixel coordinate system is defined in terms of this physical pixel size. The nominal focal length of the mirror is then needed to convert to actual angular size. (In practice, the angular size may be directly encoded in a WCS CDELT header parameter).

The Tangent Plane pixel coordinates are defined in the same way, but form the pixel plane for the Mirror Spherical Coordinates. Specifically, we define the standard **ASC-FP-FSC-1.0** variant of focal plane coordinates as $(t_x = 1, t_y = -1)$

$$\begin{aligned} FPX &= FPX0 + \Delta_s^{-1}(Y_N/|X_N|) \\ FPY &= FPY0 - \Delta_s^{-1}(Z_N/|X_N|) \end{aligned} \tag{25}$$

Note that in the focal plane X_N is negative but we take the absolute value in the formula. The sign on FPY is then chosen to take out the mirror inversion of the image caused by the optics. The sign on FPX reflects the fact that we want celestial longitude to increase from right to left when the roll angle is zero.

To repeat this in another way: (assuming zero roll angle and the default chip orientation)

- Source moves to higher RA
- Source moves to left in sky image, so sky X decreases
- FPX decreases
- Incoming photon moves to smaller MNC Y and MNC Y/$|X|$
- Image moves to larger MNC Y, FC Y, LSI Y, CHIP X

and

- Source moves to higher Dec
- Source moves up in sky image, so sky Y increases
- FPY increases
- Incoming photon moves to larger MNC Z
- Image moves to smaller MNC Z, FC Z, LSI Z, CHIP Y

We define the standard **ASC-TP-MSC-1.0** version of tangent plane coordinates as

$$\begin{aligned} TPX &= FPX0 + \Delta_s^{-1}(Y_N/|X_N|) \\ TPY &= FPY0 - \Delta_s^{-1}(Z_N/|X_N|) \end{aligned} \tag{26}$$

(identical to the focal plane coordinates) where here the (X_N, Y_N, Z_N) are the unit vector in MNC coordinates of the incoming ray. Tangent plane coordinates are defined to apply to positions on the 'sky' side of the mirror, and do not include mirror optical distortions, while focal plane coordinates do. In practice we assume that tangent plane and focal plane coordinates are identical, and mirror distortions are handled in the spatial variation of the centroid of the PSF.

Thus in our simple mirror model where an incoming photon coming from unit vector (X, Y, Z) with ray unit vector $(-X, -Y, -Z)$ is imaged to a ray with the same unit vector $(-X, -Y, -Z)$, the tangent plane coordinates of the incoming photon TPX, TPY are equal to the focal plane coordinates of the imaged ray. For incoming rays the sign of X is always negative, so -X is positive.

For XRCF, we adopt a different convention. Instead of looking at the sky from the detector, we look at the detector from the source, choosing $t_x = t_y = -1$. Then FPX is parallel to - MNC Y or + XRCF Y; FPY is parallel to - MNC Z or + XRCF Z. Users should be aware of the difference between FP coordinates at XRCF and in flight.

Table 1: Default axis orientations

Flight	XRCF
-RA, +Dec	+XRCF Y, +XRCF Z
+FPX, +FPY	+FPX, +FPY
+MNY, -MNZ	-MNY, -MNZ
+FCY, -FCZ	-FCY, -FCZ
+LSI Y,-LSI Z	-LSI Y, -LSI Z
+CHIP X,-CHIP Y	-CHIP X, -CHIP Y

We define Mirror Spherical Coordinates (r, θ_H, ϕ_H) in terms of mirror nodal Cartesian coordi-

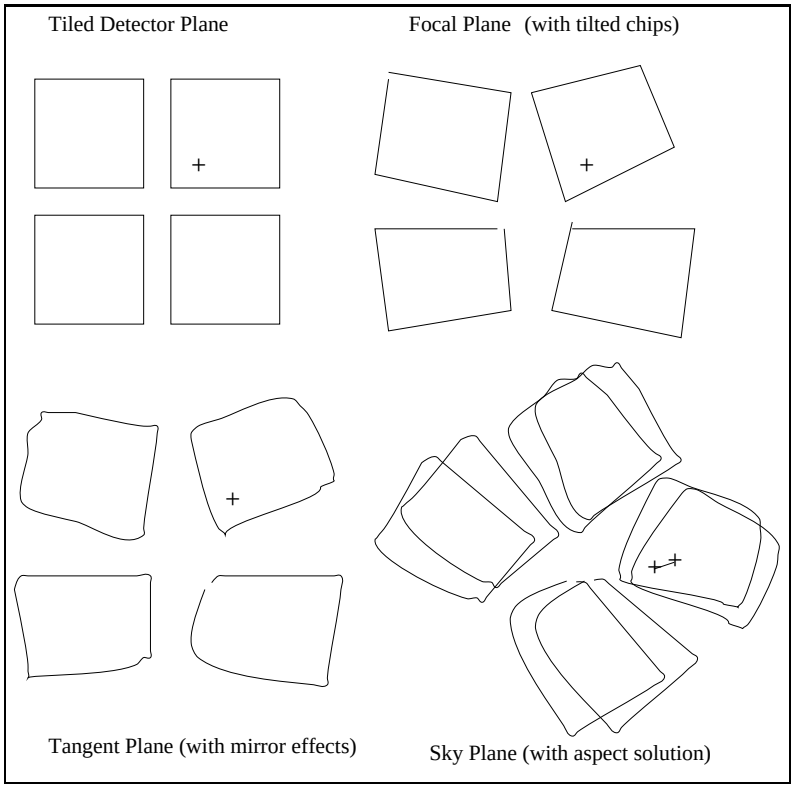

Figure 7: The different pixel plane coordinate systems. Distorting effects are highly exaggerated.

nates as follows:

$$\begin{pmatrix} X_N \\ Y_N \\ Z_N \end{pmatrix} = \begin{pmatrix} rcos\theta_H \\ r\sin\theta_H\cos\phi_H \\ r\sin\theta_H\sin\phi_H \end{pmatrix} \tag{27}$$

The angle θ_H is the **MSC off-axis angle** and ϕ_H is the **MSC Azimuth**. The inverse is

$$\begin{aligned} r &= \sqrt{X_N^2 + Y_N^2 + Z_N^2} \\ \theta_H &= \cos^{-1}(X_N/r) \\ \phi_H &= \arg(Y_N, Z_N) \end{aligned} \tag{28}$$

The Focal Surface Coordinates (r, θ_F, ϕ_F) are

$$\begin{pmatrix} X_N \\ Y_N \\ Z_N \end{pmatrix} = \begin{pmatrix} -rcos\theta_F \\ r\sin\theta_F\cos\phi_F \\ r\sin\theta_F\sin\phi_F \end{pmatrix} \tag{29}$$

The angle θ_F is the **FSC off-axis angle** and the angle ϕ_F is the **FSC azimuth**. They are related to the MSC coordinates by

$$\theta_F = \pi - \theta_H, \quad \phi_F = \phi_H \tag{30}$$

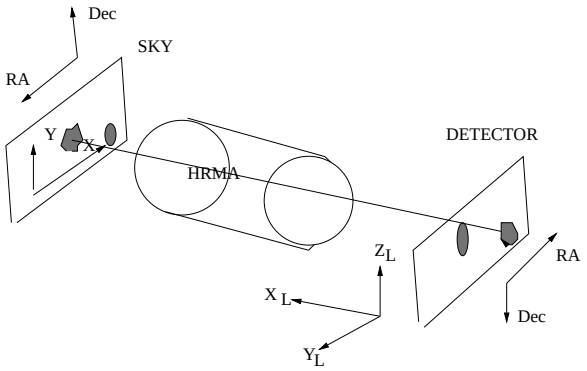

Figure 8: Imaging the sky in LSI coordinates

The inverse is

$$\begin{aligned} r &= \sqrt{X_N^2 + Y_N^2 + Z_N^2} \\ \theta_H &= \cos^{-1}(-X_N/r) \\ \phi_H &= \arg(Y_N, Z_N) \end{aligned} \tag{31}$$

2.2.5 Pixel planes for intermediate systems

We may want to make pixel images for data in coordinate systems such as LSI and STF frames. To do this we use the FP system and set the LSI or STF origin at the nominal focus by specifying a physical pixel size. ASC-FP-STF-1.0 coordinates are like ASC-FP-FSC-1.0 coordinates but ignore the possibility of defocus or misalignment (or dither) between the instrument compartment and the mirrors. ASC-FP-LSI-1.0 coordinates further ignore the possibility that the the instrument is not at its standard position in the focus (no SI instrument table correction) while ASC-FP-STT-1.0 coordinates artificially place the STT origin at the focus. For each of these systems,

$$\begin{aligned} FPX &= FPX0 + \Delta_{sp}^{-1} Y \\ FPY &= FPY0 - \Delta_{sp}^{-1} Z \end{aligned} \tag{32}$$

where Δ_{sp} is the physical pixel size and Y,Z are the LSI, STT, etc., coordinates, while the X-coordinate is ignored.

The ASC-FP-STF-1.0 pixel coordinate system is also called 'dithered focal plane coordinates' since it can be used to debug XRCF dither mode.

2.3 Data Analysis 2: Tangent Plane to Sky

2.3.1 Sky Pixel Coordinates

The Sky Pixel coordinate system is a translation and rotation of the Tangent Plane pixel coordinate system to align the image with a nominal pointing direction and spacecraft roll angle. For small aspect corrections, sky pixel coordinates (ASC-SKY-1.0) are

$$\begin{aligned} X &= FPX0 + (TPX - FPX0)\cos\gamma - (TPY - FPY0)\sin\gamma + A_X \\ Y &= FPY0 + (TPX - FPX0)\sin\gamma + (TPY - FPY0)\cos\gamma + A_Y \end{aligned} \tag{33}$$

The quantities A_X and A_Y are the sky frame aspect offsets in pixels, determining the sky pixel coordinates of the optical axis. (Note that the aspect offsets for Einstein and Rosat were stored as detector frame offsets, which required applying the roll angle to; it's not clear to me why this choice was made.)

In general when combining data over a wide range of pointing directions, (mosaicing images) we must reproject to the nominal sky tangent plane.

2.3.2 Physical Tangent Plane coordinates

If the Tangent Plane pixel coordinates represent a position on the tangent plane to the unit sphere at the optical axis, the Physical Tangent Plane coordinate system

$$\begin{pmatrix} X_{PTP} \\ Y_{PTP} \\ Z_{PTP} \end{pmatrix} = \begin{pmatrix} -\Delta_s(TPX - TPX0) \\ \Delta_s(TPY - TPY0) \\ 1 \end{pmatrix}. \tag{34}$$

represents the 3D vector from the center of the unit sphere to that position on the tangent plane, which the convention that the X_{PTP} and Y_{PTP} axes run in the direction of increasing RA and Dec respectively in the on-orbit case with zero roll. The PTP system is closely related to HRMA Nodal coordinates. If the direction of the incoming ray is (X_N, Y_N, Z_N) then

$$\begin{pmatrix} X_{PTP} \\ Y_{PTP} \\ Z_{PTP} \end{pmatrix} = \begin{pmatrix} Y_N/X_N \\ Z_N/X_N \\ 1 \end{pmatrix} \tag{35}$$

2.3.3 Physical Sky Plane coordinates

The Physical Sky Plane coordinate system for zero aspect offset and finite roll angle is

$$\begin{pmatrix} X_{PSP} \\ Y_{PSP} \\ Z_{PSP} \end{pmatrix} = \begin{pmatrix} X_{PTP}\cos\gamma + Y_{PTP}\sin\gamma \\ X_{PTP}\sin\gamma - Y_{PTP}\cos\gamma \\ Z_{PTP} \end{pmatrix} \tag{36}$$

where γ is the spacecraft roll angle.

The PTP and PSP systems are important as you need them to calculate the RA and Dec. However they are only used in internal calculations.

2.3.4 J2000 Celestial Coordinates

One can go from Tangent Plane Physical coordinates to J2000 celestial coordinates using the instantaneous pointing direction (α_A, δ_A). and roll angle γ_A.

$$\mathcal{S}(\alpha,\delta) = \mathrm{Rot}(\pi/2+\gamma_A, \pi/2-\delta_A, \pi-\alpha_A) \begin{pmatrix} X_{PTP} \\ Y_{PTP} \\ Z_{PTP} \end{pmatrix} \tag{37}$$

Use the nominal pointing direction (α_0, δ_0) and set the roll angle to zero if using Sky Plane Physical Coordinates:

$$\mathcal{S}(\alpha,\delta) = \mathrm{Rot}(\pi/2, \pi/2-\delta_0, \pi-\alpha_0) \begin{pmatrix} X_{PSP} \\ Y_{PSP} \\ Z_{PSP} \end{pmatrix} \tag{38}$$

From TP pixel coordinates, recall that

$$\begin{pmatrix} X_{PTP} \\ Y_{PTP} \\ Z_{PTP} \end{pmatrix} = \begin{pmatrix} -\Delta_s(TPX - TPX0) \\ \Delta_s(TPY - TPY0) \\ 1 \end{pmatrix} \tag{39}$$

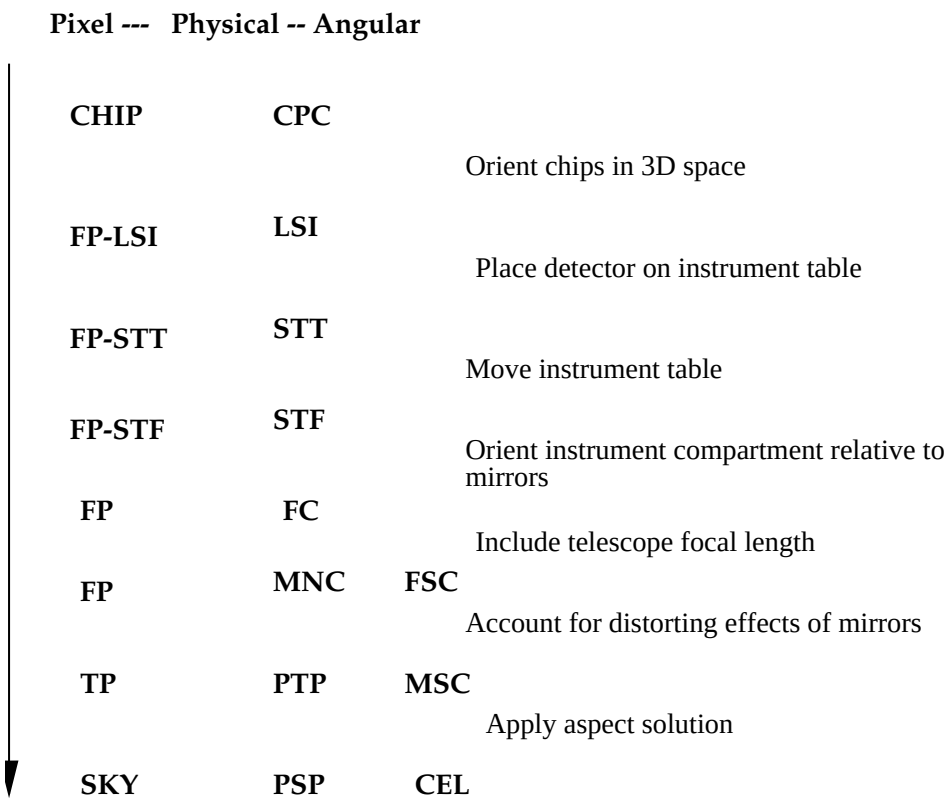

Figure 9: Coordinate systems used in data analysis, 1: Imaging data analysis.

2.4 Simulation: Sky to Telemetry

2.4.1 Mirror Spherical Coordinates to Focal Surface Coordinates

Incoming photons with given mirror spherical coordinates (off axis angle and azimuth) can be described by their tangent plane pixel coordinates. To first order, these are the same as the focal plane pixel coordinates; determining the higher order corrections is the job of ray trace simulators such as SAOSAC. When simulating, we often will not bother with these tangent and pixel plane coordinates but instead will work directly with mirror nodal coordinates.

2.4.2 Focal Surface or Mirror Nodal Coordinates to CPC coordinates

We then have the problem: how to transform from mirror nodal coordinates of a ray emerging from the mirror to the detected photon position. This is harder than working in the data analysis direction. We choose a Cartesian coordinate system (usually LSI coordinates) and calculate the intersection of the ray line with each detector plane. There should be only one detector plane which has an intersection within its finite bounds (i.e., the photon will only hit one of the chips). For

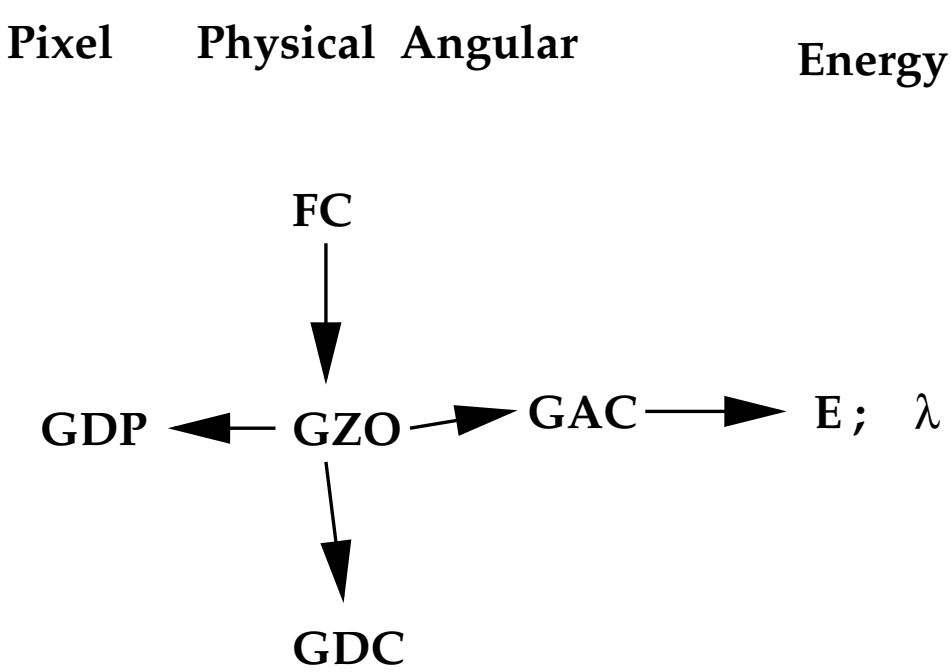

Figure 10: Coordinate systems used in data analysis, 2: Grating data analysis.

detectors which do not include any tilted or out-of-plane chips (pre-AXAF missions), the calculation is much easier as you can just find the LSI coordinates of the ray when it hits the focal plane.

In our more complicated situtation, as before a general point on one of the detector planes is

$$\boldsymbol{r} = \boldsymbol{p_0} + X_{CPC}\boldsymbol{e}_X + Y_{CPC}\boldsymbol{e}_Y \tag{40}$$

where $\boldsymbol{p_0}$ is the origin of CPC coordinates, and $\boldsymbol{e}_X$ and $\boldsymbol{e}_Y$ are the unit vectors along the CPC axes, with $\boldsymbol{e}_Z$ as the unit normal to the plane.

The general ray is

$$\boldsymbol{r} = \boldsymbol{l_0} + \lambda \boldsymbol{l} \tag{41}$$

where $\boldsymbol{l_0}$ is an arbitrary point on the ray (the output of ray trace or else for approximate calculations, the mirror node), $\boldsymbol{l}$ is the ray direction, and λ labels positions along the ray. The intersection with the plane is then at

$$\boldsymbol{r} = \boldsymbol{l_0} + \frac{(\boldsymbol{p_0} - \boldsymbol{l_0}).\boldsymbol{e}_Z}{\boldsymbol{l}.\boldsymbol{e}_Z}\boldsymbol{l} \tag{42}$$

and we find CPC X and Y by taking the dot product with the CPC unit vectors,

$$X_{CPC} = \boldsymbol{r}.\boldsymbol{e}_X, \quad Y_{CPC} = \boldsymbol{r}.\boldsymbol{e}_Y \tag{43}$$

2.4.3 Chip coordinates

We can then recover chip coordinates and telemetry coordinates using the equations from previous sections.

$$\begin{aligned} CHIPX &= X_{CPC}/\Delta_p + 0.5 \\ CHIPY &= Y_{CPC}/\Delta_p + 0.5 \end{aligned} \tag{44}$$

2.5 Summary of coordinate systems

Each of the physical coordinate systems, representing either a 3-D position or a 2-D angular position, has a corresponding 2-D pixel coordinate system used for display purposes and for practical storage in cases where the third dimension is redundant.

In the following table, I give each physical system with the corresponding pixel plane systems. 'Label' is the generic label used to identify the system; data associated with this label is deemed to satisfy the equations in this document, and revisions to the equations will imply version number changes in the label. To isolate a specific system, extra parameters such as the chip ID are required. The table also notes whether information is lost going from the physical to the pixel system.

Physical System	Name	Pixel System	Params	Info Loss	Description
CPC	Chip Physical	ASC-CHIP-1.0	Inst. ID, Chip ID	No	Single chip
CPC	Chip Physical	ASC-TDET-1.0	Inst. ID, TDET params	No	Detector coords
LSI	Local SI	ASC-FP-LSI-1.0	Inst. ID	Yes	Focal plane, offset uncc
STT	SI Translation Table	ASC-FP-STT-1.0	Pixel size	Yes	Focal plane, offset uncc
STF	SI Translation Frame	ASC-FP-STF-1.0	Pixel size	Yes	Focal plane, alignment
FC	Focus Coordinates	ASC-FP-FSC-1.0	Pixel size	Yes	Focal plane
MNC	Mirror Nodal	ASC-FP-FSC-1.0	Pixel size	Yes	Focal plane
FSC	Focal Surface	ASC-FP-FSC-1.0	Pixel size	No	Focal plane
MNC	Mirror Nodal	ASC-TP-MSC-1.0	Pixel size	Yes	Tangent plane
MSC	Mirror Spherical	ASC-TP-MSC-1.0	Pixel size	No	Tangent plane
CEL	Celestial	ASC-SKY-1.0	Pixel size	No	Aspect applied
PTP	Physical Tangent Plane	ASC-TP-MSC-1.0	Pixel size	No	Tangent Plane 3D
PSP	Physical Sky Plane	ASC-SKY-1.0	Pixel size	No	Sky Plane 3D

The TDET parameters for tiled detector coordinates are arbitrary, so there can be several parallel TDET systems for one instrument and individual TDET labels assigned for each system must be used.

The pixel size used in the FP and TP systems is often equal to the detector pixel size in the nominal focal plane, but sometimes is picked arbitrarily.

3 Data Analysis Coordinate Systems - Gratings

We now consider objective transmission gratings placed between the mirrors and the detectors.

3.1 Data Analysis: Grating data

When we observe with the gratings, we get a dispersed spectrum with orders +1, -1, +2, -2, ... and a zero-order undispersed image. The undispersed (zero-order) photons do not interact with the gratings and we can deal with them using the same analysis as for imaging detectors. To analyse a dispersed photon, however, we must know the location of the zero-order image as well as that of the dispersed photon. For instance, spacecraft roll aspect must be applied to the zero-order position, not the dispersed position.

The location of the zero order photon must be calculated relative to the Grating Node rather than the Mirror Node. The Grating Node is on the optical axis at a distance R from the focus, where R is the diameter of the Rowland Circle.

Each grating is defined by a grating node position and a grating pole vector which defines the cross-dispersion direction.

3.1.1 Grating Zero Order Coordinates (GZO-1.0)

Now we pick a source, with zero order position $\boldsymbol{ZO}$. and let the vector from the grating node to the source zero order be $\boldsymbol{S}$. Then define

$$\begin{aligned} \boldsymbol{e}_{X_{ZO}} &= -\boldsymbol{S}/|\boldsymbol{S}| \\ \boldsymbol{e}_{Y_{ZO}} &= \boldsymbol{d_0} \wedge \boldsymbol{e}_{X_{ZO}}/|\boldsymbol{d_0} \wedge \boldsymbol{e}_{X_{ZO}}| \\ \boldsymbol{e}_{Z_{ZO}} &= \boldsymbol{e}_{X_{ZO}} \wedge \boldsymbol{e}_{Y_{ZO}} \end{aligned} \tag{45}$$

where the Grating Pole (cross-dispersion unit vector) $\boldsymbol{d_0}$ is

$$\boldsymbol{d_0} = (0, -\sin\alpha_G, \cos\alpha_G) \tag{46}$$

in MNC coordinates, where α_G is the angle between the dispersion direction and the spacecraft Y axis.

This defines a cartesian orthonormal set, Grating Zero Order Coordinates, whose origin we choose to be at $\boldsymbol{G0}$. Diffracted photons travel in the X_{ZO}, Y_{ZO} plane, and the intersection of this plane with the detector surface defines the dispersion direction.

The key step is calculating the GZO to FC transformation matrix. The columns of this matrix are simply the vectors $\boldsymbol{e}_{X_{Z0}}$ etc.

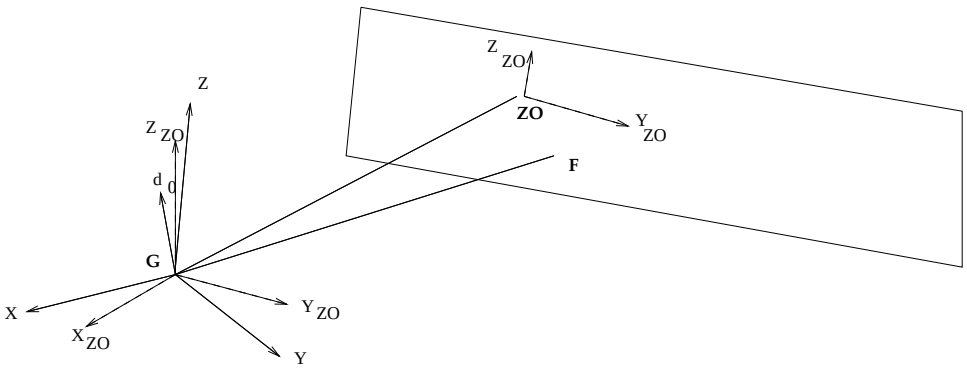

Figure 11: Grating Zero Order coordinates

The GZO coordinates of the photon are then

$$P(GZO) = R(FC, GZO)(P(FC) - O_{GZO}(FC)) \tag{47}$$

where $O_{GZO}(LSI)$ are the FC coordinates of the grating node.

For an approximate treatment (which can be in error by several pixels), we can write the zero order coords as

$$ZO(FC) = (X, Y, Z) = (gX_o, gY_o, gZ_o) \tag{48}$$

where g is the distance from G0 to the focus. Then to first order

$$|S| = g(1 - X_o) \tag{49}$$

and

$$\begin{aligned} \boldsymbol{e}_{X_{ZO}} &= (1, -Y_o, -Z_o) \\ \boldsymbol{e}_{Y_{ZO}} &= ((Z_o \sin\alpha_G + Y_o \cos\alpha_G), \cos\alpha_G, \sin\alpha_G) \\ \boldsymbol{e}_{Z_{ZO}} &= (-Y_o \sin\alpha_G + Z_o \cos\alpha_G, -\sin\alpha_G, \cos\alpha_G) \end{aligned} \tag{50}$$

so that a point with FC coords (x, y, z) will have GZO coords

$$P(GZO) = (x - g, (y - Y)\cos\alpha_G + (z - Z)\sin\alpha_G, (z - Z)\cos\alpha_G - (y - Y)\sin\alpha_G) \tag{51}$$

3.1.2 Grating Angular Coordinates (GAC-1.0)

Grating Angular Coordinates (GAC) are the most important system for grating analysis. The GAC system (θ_r, θ_d) is a 2D angular system giving longitude and latitude with respect to GZO coordinates. The longitude coordinate, θ_r, is the **dispersion angle** and the latitude coordinate, θ_d, is the **cross-dispersion** angle. They are defined as

$$\begin{aligned} \theta_r &= \tan^{-1}\left(\frac{-Y_{ZO}}{X_{ZO}}\right) && \sim -Y_{ZO}/X_{ZO} \\ \theta_d &= \tan^{-1}\left(\frac{+Z_{ZO}}{\sqrt{X_{ZO}^2 + Y_{ZO}^2}}\right) && \sim +Z_{ZO}/X_{ZO} \end{aligned} \tag{52}$$

3.1.3 Grating Diffraction Coordinates (GDC-1.0)

The Grating Diffraction Coordinate system (r_{TG}, d_{TG}) gives the distance in mm along the dispersion direction and in the cross-dispersion direction. This is just related to the GAC coordinates by a simple scaling

$$\begin{aligned} r_{TG} &= X_R \theta_r \\ d_{TG} &= X_R \tan\theta_d \end{aligned} \tag{53}$$

Here X_R is the length from the grating node to the focus, which is approximately equal to the length $|\boldsymbol{S}|$.

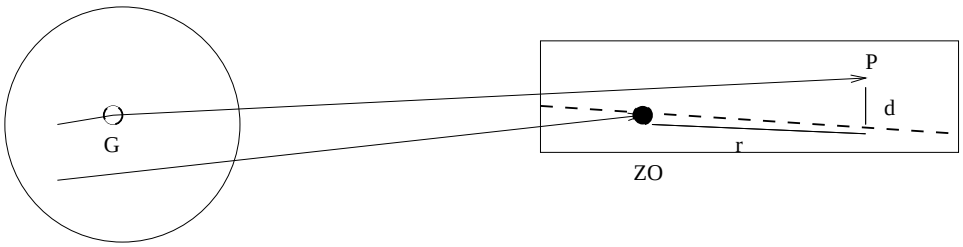

Figure 12: Grating Diffraction coordinates

3.1.4 Grating Diffraction Plane Pixel Coordinates (GDP-1.1)

The Grating Diffraction Plane Pixel Coordinates GDX, GDY are defined by

$$\begin{aligned} GDX &= GDX0 - \Delta_{gs}^{-1}(Y_{ZO}/X_{ZO}) \\ GDY &= GDY0 + \Delta_{gs}^{-1}(Z_{ZO}/X_{ZO}) \end{aligned} \tag{54}$$

analogously to the Focal Plane Pixel Coordinates.

They are related to the physical Grating Diffraction Coordinates by

$$\begin{aligned} GDX &= GDX0 + \Delta_{gs}^{-1}\tan(r_{TG}/X_R) \\ GDY &= GDY0 + \Delta_{gs}^{-1}(d_{TG}/X_R)\cos(r_{TG}/X_R) \end{aligned} \tag{55}$$

3.1.5 Dispersion relation

The wavelength of the diffracted photon is

$$\lambda = P\sin\theta_R/m \tag{56}$$

where P is the average grating period and m is the diffraction order. So

$$\lambda \sim (P/m)(GDX - GDX0)\Delta_{gs} \tag{57}$$

Part II
Part 2: AXAF systems

4 ACIS

4.1 Instrumental details

The ACIS instrument has 10 CCD chips. In the event list data, each is identified by an integer from 0 to 9. Four of the chips, the imaging set, are arranged in a rough square (but individually tilted). Six are the spectroscopic array, arranged in a line.

Chip Name	CHIP ID
ACIS-I0	0
ACIS-I1	1
ACIS-I2	2
ACIS-I3	3
ACIS-S0	4
ACIS-S1	5
ACIS-S2	6
ACIS-S3	7
ACIS-S4	8
ACIS-S5	9

The CHIP ID is also called CCD ID for consistency with ASCA.

4.1.1 ACIS readout coordinates

The ACIS readout coordinate system was explained in a 1995 draft memo from J Woo. This memo defines two coordinate systems, the "pixel coordinate system of the readout file array, f(x,y)", which I will call the **ACIS Readout Coordinates** $(XREAD, YREAD)$ with identifier AXAF-ACIS-3.0, and the "pixel coordinate system of the active detector image array p(x,y)", which I will call **ACIS Chip Coordinates**, $(XCHIP, YCHIP)$ with identifier AXAF-ACIS-1.0 (these are the ones that run from 1 to 1024).

ACIS Readout Coordinates may be seen in subassembly cal (SAC) data, but in flight the Chip coordinates are calculated on board and telemetered directly. We don't normally deal with the readout coordinates.

The two systems are related by

$$YCHIP = \begin{cases} YREAD & 1 \le YREAD \le 1026 \\ \text{Overclock} & 1027 \le YREAD \le 1030 \end{cases} \quad (58)$$

$$XCHIP = \begin{cases} \text{Underclock} & 1 \le XREAD \le 4 & \\ XREAD - 4 & 5 \le XREAD \le 260 & \text{(Node A)} \\ \text{Overclock} & 261 \le XREAD \le 337 & \\ \text{Undefined Parallel Transfer} & 338 \le XREAD \le 340 & \\ \text{Underclock} & 341 \le XREAD \le 344 & \\ 857 - XREAD & 345 \le XREAD \le 600 & \text{(Node B} \\ \text{Overclock} & 601 \le XREAD \le 677 & \\ \text{Undefined Parallel Transfer} & 678 \le XREAD \le 680 & \\ \text{Underclock} & 681 \le XREAD \le 684 & \\ XREAD - 172 & 685 \le XREAD \le 940 & \text{(Node C)} \\ \text{Overclock} & 941 \le XREAD \le 1017 & \\ \text{Undefined Parallel Transfer} & 1018 \le XREAD \le 1020 & \\ \text{Underclock} & 1021 \le XREAD \le 1024 & \\ 2049 - XREAD & 1025 \le XREAD \le 1280 & \text{(Node D)} \\ \text{Overclock} & 1281 \le XREAD \le 1357 & \\ \text{Undefined Parallel Transfer} & 1358 \le XREAD \le 1360 & \end{cases} \tag{59}$$

The inverse transformation is

$$\begin{aligned} YREAD &= YCHIP \\ XREAD &= \begin{cases} XCHIP + 4 & 1 \le XCHIP \le 256 & \text{(A)} \\ 857 - XCHIP & 257 \le XCHIP \le 512 & \text{(B)} \\ XCHIP + 172 & 513 \le XCHIP \le 768 & \text{(C)} \\ 2049 - XCHIP & 769 \le XCHIP \le 1024 & \text{(D)} \end{cases} \end{aligned} \tag{60}$$

Unresolved questions: Is the above correct, or even useful? Do the telemetry values start at 1 or 0? Under what circumstances do we get YCHIP values of 1025 and 1026? Do those values correspond to true active area?

4.1.2 ACIS Fast Window mode

In window mode, we get an initial set of Window Chip Coordinates (AXAF-ACIS-4.0) WX, WY which run from 1 to 1024 and 1 to WSIZE. WSIZE is a configurable number.

There is no way to uniquely know from the telemetry what the true ACIS chip coordinates of the photon were - you get an uncertainty module WSIZE. However, to calculate best guess ACIS chip coordinates (AXAF-ACIS-1.0) we can assume that the photon is associated with a known incident source location, resolving the uncertainties.

For non grating data, calculate the predicted AXAF-ACIS-1.0 coordinates for the incident radiation, say (CX0, CY0). At XRCF, this will involve the forward calculation including the STF coordinates of the FAM. Then set

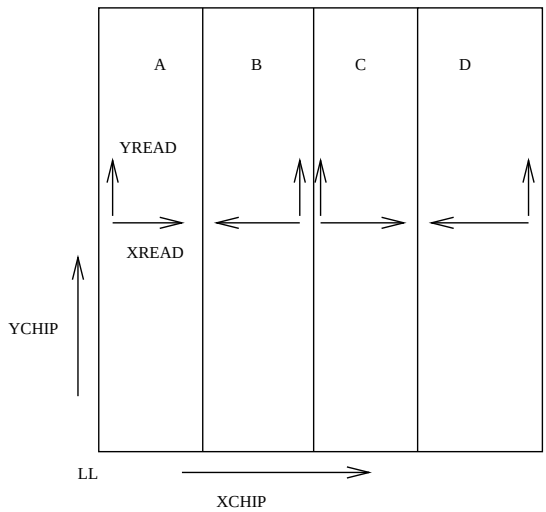

Figure 13: ACIS readout nodes

```
CY1 = (CY0 / WSIZE ) * WSIZE
```

using integer arithmetic. Then

$$CHIPX = WX \tag{61}$$

and

$$CHIPY = WY + CY1 \tag{62}$$

4.2 2-D detector coordinates: TDET parameters

The ASC-TDET-1.0 tiled detector coordinates are implemented for AXAF with the following specific systems, each of which specifies a TDET system in terms of the CHIP coordinates.

Table 4: Tiled Detector Plane systems

System	Size	X Center, Y Center	Use
AXAF-ACIS-2.2	8192 x 8192	(4096.5, 4096.5)	Standard
AXAF-ACIS-2.3A	32768x32768	(16384.5, 16384.5)	Obsolete

Table 5: Parameters of Tiled Detector Coordinate definitions

Tiled System	Chip	θ_i	Δ_i	$X0_i$	$Y0_i$	H_i
AXAF-ACIS-2.2	ACIS-I0	90	1	3061.0	5131.0	1
AXAF-ACIS-2.2	ACIS-I1	270	1	5131.0	4107.0	1
AXAF-ACIS-2.2	ACIS-I2	90	1	3061.0	4085.0	1
AXAF-ACIS-2.2	ACIS-I3	270	1	5131.0	3061.0	1
AXAF-ACIS-2.2	ACIS-S0	0	1	791.0	1702.0	1
AXAF-ACIS-2.2	ACIS-S1	0	1	1833.0	1702.0	1
AXAF-ACIS-2.2	ACIS-S2	0	1	2875.0	1702.0	1
AXAF-ACIS-2.2	ACIS-S3	0	1	3917.0	1702.0	1
AXAF-ACIS-2.2	ACIS-S4	0	1	4959.0	1702.0	1

AXAF-ACIS-2.3A	ACIS-S2	0	5	11220.0	8510.0	1
AXAF-ACIS-2.3A	ACIS-S3	0	5	16430.0	8510.0	1
AXAF-ACIS-2.3A	ACIS-S4	0	5	21640.0	8510.0	1
AXAF-ACIS-2.3A	ACIS-S5	0	5	26850.0	8510.0	1

4.3 3-D chip locations: CPC to LSI transformation parameters

In the following tables we list the CPC and LSI coordinates of each corner of each chip. We give coordinates for each of the ACIS chips in both the ACIS-I and ACIS-S LSI systems, since we may take data from ACIS-S chips while ACIS-I is in the focus or vice versa. The systems are simply offset by 46.88mm in the Z_{LSI} direction. The ACIS data is from ACIS-SOP-01, and the HRC data is deduced from information provided by M. Juda.

Table 6: ACIS Chip corner locations in ACIS-I LSI coordinates

Chip	Corner	CPC coords	ACIS-I LSI coords
I0	LL	(0.0, 0.0, 0.0)	(2.361, -26.484, 23.088)
	LR	(24.58, 0.0, 0.0)	(1.130, -26.546, -1.458)
	UR	(24.58, 24.58, 0.0)	(-0.100, -2.001, -1.458)
	UL	(0.0, 24.58, 0.0)	(1.130, -1.939, 23.088)
I1	LL	(0.0, 0.0, 0.0)	(1.130, 23.086, -1.458)
	LR	(24.58, 0.0, 0.0)	(2.360, 23.024, 23.088)
	UR	(24.58, 24.58, 0.0)	(1.130, -1.521, 23.088)
	UL	(0.0, 24.58, 0.0)	(-0.100, -1.459, -1.458)
I2	LL	(0.0, 0.0, 0.0)	(1.130, -26.546, -1.997)
	LR	(24.58, 0.0, 0.0)	(2.361, -26.484, -26.543)
	UR	(24.58, 24.58, 0.0)	(1.130, -1.939, -26.543)
	UL	(0.0, 24.58, 0.0)	(-0.100, -2.001, -1.997)
I3	LL	(0.0, 0.0, 0.0)	(2.361, 23.024, -26.543)
	LR	(24.58, 0.0, 0.0)	(1.131, 23.086, -1.997)
	UR	(24.58, 24.58, 0.0)	(-0.100, -1.459, -1.997)
	UL	(0.0, 24.58, 0.0)	(1.130, -1.521, -26.543)
S0	LL	(0.0, 0.0, 0.0)	(0.744, -81.051, -59.170)
	LR	(24.58, 0.0, 0.0)	(0.353, -56.478, -59.170)
	UR	(24.58, 24.58, 0.0)	(0.353, -56.478, -34.590)
	UL	(0.0, 24.58, 0.0)	(0.744, -81.051, -34.590)
S1	LL	(0.0, 0.0, 0.0)	(0.348, -56.047, -59.170)
	LR	(24.58, 0.0, 0.0)	(0.099, -31.473, -59.170)
	UR	(24.58, 24.58, 0.0)	(0.099, -31.473, -34.590)
	UL	(0.0, 24.58, 0.0)	(0.348, -56.047, -34.590)
S2	LL	(0.0, 0.0, 0.0)	(0.096, -31.042, -59.170)
	LR	(24.58, 0.0, 0.0)	(-0.011, -6.466, -59.170)
	UR	(24.58, 24.58, 0.0)	(-0.011, -6.466, -34.590)
	UL	(0.0, 24.58, 0.0)	(0.096, -31.042, -34.590)
S3	LL	(0.0, 0.0, 0.0)	(-0.011, -6.035, -59.170)
	LR	(24.58, 0.0, 0.0)	(0.024, 18.541, -59.170)
	UR	(24.58, 24.58, 0.0)	(0.024, 18.541, -34.590)

	UL	(0.0, 24.58, 0.0)	(-0.011, -6.035, -34.590)
S4	LL	(0.0, 0.0, 0.0)	(0.026, 18.972, -59.170)
	LR	(24.58, 0.0, 0.0)	(0.208, 43.547, -59.170)
	UR	(24.58, 24.58, 0.0)	(0.208, 43.547, -34.590)
	UL	(0.0, 24.58, 0.0)	(0.026, 18.972, -34.590)
S5	LL	(0.0, 0.0, 0.0)	(0.208, 43.978, -59.170)
	LR	(24.58, 0.0, 0.0)	(0.528, 68.552, -59.170)
	UR	(24.58, 24.58, 0.0)	(0.528, 68.552, -34.590)
	UL	(0.0, 24.58, 0.0)	(0.208, 43.978, -34.590)

5 HRC

5.1 Overview

The HRC instrument has two detectors, the HRC-S and the HRC-I. The HRC-I has a single 'chip' or microchannel plate pair (CHIP ID = 0, name HRC-I) while the HRC-S has three (CHIP ID = 1,2,3; name HRC-S1,S2,S3; HRC team

designation +1, 0, -1). We define an HRC-I chip plane which is 16384 pixels square; (not all of these pixels correspond to actual readable values); the HRC-S chips are 4096 x 16384, 4096 x 15872, and 4096 x 16384 pixels respectively. The HRC-I pixel size is 0.006429 mm; however, the HRC-S pixels are actually rectangular, with the U axis size 0.006250 mm and the V axis size 0.006429 mm.

Name	ID	CHIP size (pix)	Pixel size (μ)	CHIP size (mm)
HRC-I	0	16384 x 16384	6.429 x 6.429	105.333 x 105.333
HRC-S1	1	4096 x 16384	6.250 x 6.429	25.600 x 105.333
HRC-S2	2	4096 x 15872	6.250 x 6.429	25.600 x 102.041
HRC-S3	3	4096 x 16384	6.250 x 6.429	25.600 x 105.333

5.1.1 3-D chip locations: CPC to LSI parameters

The corners of these logical chip planes are located in the LSI coordinate system as follows; these are calculated by placing the HRC-S origin (default aimpoint) at 4.0mm to +LSI Y of the detector center and using the chip sizes calculated above together with the designed S1 and S3 chip tilts in the X,Y plane.

Table 8: HRC chip (i.e. grid) corner locations in LSI coordinates

Chip	Corner	CPC coords	HRC-I,S LSI coords
HRC-I	LL	(0.000 , 0.000 , 0.000)	(0.000 , 0.000 , 74.482)
HRC-I	LR	(105.333 , 0.000 , 0.000)	(0.000 , 74.482 , 0.000)

HRC-I	UR	(105.333 , 105.333 , 0.000)	(0.000 , 0.000 , -74.482)
HRC-I	UL	(0.000 , 105.333 , 0.000)	(0.000 , -74.482 , 0.000)
HRC-S1	LL	(0.000 , 0.000 , 0.000)	(2.622 , 160.320 , -12.800)
HRC-S1	LR	(25.600 , 0.000 , 0.000)	(2.622 , 160.320 , 12.800)
HRC-S1	UR	(25.600 , 105.333 , 0.000)	(0.000 , 55.020 , 12.800)
HRC-S1	UL	(0.000 , 105.333 , 0.000)	(0.000 , 55.020 , -12.800)
HRC-S2	LL	(0.000 , 0.000 , 0.000)	(0.000 , 55.020 , -12.800)
HRC-S2	LR	(25.600 , 0.000 , 0.000)	(0.000 , 55.020 , 12.800)
HRC-S2	UR	(25.600 , 102.041 , 0.000)	(0.000 , -47.020 , 12.800)
HRC-S2	UL	(0.000 , 102.041 , 0.000)	(0.000 , -47.020 , -12.800)
HRC-S3	LL	(0.000 , 0.000 , 0.000)	(0.000 , -47.020 , -12.800)
HRC-S3	LR	(25.600 , 0.000 , 0.000)	(0.000 , -47.020 , 12.800)
HRC-S3	UR	(25.600 , 105.333 , 0.000)	(2.248 , -152.320 , 12.800)
HRC-S3	UL	(0.000 , 105.333 , 0.000)	(2.248 , -152.320 , -12.800)

5.1.2 2-D detector coordinates: TDET parameters

The ASC-TDET-1.0 tiled detector coordinates are implemented for AXAF with the following specific systems, each of which specifies a TDET system in terms of the CHIP coordinates.

Table 9: Tiled Detector Plane systems

System	Size	X Center, Y Center	Use
AXAF-HRC-2.3I	16384 x 16384	(8192.5, 8192.5)	Standard HRC-I
AXAF-HRC-2.4S	16384 x 16384	(8192.5, 8192.5)	Standard HRC-S
AXAF-HRC-2.2I	32768 x 32768	(16384.5, 16384.5)	Alternative
AXAF-HRC-2.2S	49152 x 4096	(24576.5, 2048.5)	Incorrect, 2.5S replaces
AXAF-HRC-2.3S	16384 x 24976	(8192.5, 12488.5)	Obsolete
AXAF-HRC-2.5S	49152 x 4096	(24576.5, 2048.5)	Alternative

Table 10: Parameters of Tiled Detector Coordinate definitions

Tiled System	Chip	θ_i	Δ_i	$X0_i$	$Y0_i$	H_i

AXAF-HRC-2.3I	HRC-I	90	1	0.0	0.0	-1
AXAF-HRC-2.4S	HRC-S1	270	1	16384.0	1024.0	1
AXAF-HRC-2.4S	HRC-S2	270	1	16128.0	6144.0	1
AXAF-HRC-2.4S	HRC-S3	270	1	16384.0	11264.0	1
AXAF-HRC-2.2I	HRC-I	315	1	16384.0	27969.2375	-1
AXAF-HRC-2.5S	HRC-S1	270	1	48896.0	0.0	1
AXAF-HRC-2.5S	HRC-S2	270	1	32512.0	0.0	1
AXAF-HRC-2.5S	HRC-S3	270	1	16640.0	0.0	1
AXAF-HRC-2.3S	HRC-S1	270	1	16384.0	9216.0	1
AXAF-HRC-2.3S	HRC-S2	270	1	16384.0	14336.0	1
AXAF-HRC-2.3S	HRC-S3	270	1	16384.0	19456.0	1

5.2 Instrumental details

5.2.1 HRC physical layout and Tap Coordinates (HRC-6.0)

Each HRC sub-instrument contains a series of electrical 'taps' on each axis of the wire grid, which define a continuous spatial system. The electrical axes are labelled u and v, and we will say there are N_u and N_v taps on each axis, numbered starting at 0. In the internal HRC-S electronics the three MCPs have individually numbered taps but these are combined before we see it in the telemetry. The coarse tap positions are modified by a fine position which runs from -0.5 to +0.5. Then we can define an **HRC Tap Coordinate System** (AXAF-HRC-6.0) which runs from $u = -0.5$ to $u = N_u - 0.5$, and $v = -0.5$ to $N_v - 0.5$.

5.2.2 Deriving linear tap coordinates from HRC telemetry

The instrument electronics records four numbers per axis for each event: the 'center tap' (usually the tap with the maximum voltage), and the voltages of that tap and the one on either side. These numbers, which are the values which get coded into flight telemetry, we will refer to as **HRC**

telemetry coordinates $(\mathbf{u}_{ht}, \mathbf{v}_{ht})$. The four integer components of $\mathbf{u}_{ht}$ are

$$\mathbf{u}_{ht} = \begin{cases} u_0 & \text{Max tap, 0 to } N_u - 1 \text{ ('coarse position')} \\ \text{ADC1} & \text{Voltage of } u_{\text{coarse}} - 1 \\ \text{ADC2} & \text{Voltage of } u_{\text{coarse}} \\ \text{ADC3} & \text{Voltage of } u_{\text{coarse}} + 1 \end{cases} \tag{63}$$

and similarly for $\mathbf{v}_{ht}$). From the telemetry coordinates we can calculate an intermediate quantity, the **fine position**

$$u_{\text{fine}} = \frac{\text{ADC3} - \text{ADC1}}{\text{ADC1} + \text{ADC2} + \text{ADC3}} \tag{64}$$

Note that

$$-0.5 \leq u_{\text{fine}} \leq +0.5 \tag{65}$$

We now split off the sign of this fine position correction to obtain the tap side

$$s_u = \begin{cases} +1 & (u_{\text{fine}} \geq 0) \\ -1 & (u_{\text{fine}} < 0) \end{cases} \tag{66}$$

and the fine position magnitude

$$\Delta u = |u_{\text{fine}}| \tag{67}$$

From these we calculate the linear HRC Tap Coordinates

$$\begin{aligned} u &= u_0 + s_u C_{u1}(u_0, s_v)\Delta u - s_u C_{u2}(u_0, s)\Delta u^2 \\ v &= v_0 + s_v C_{v1}(v_0, s_v)\Delta v - s_v C_{v2}(v_0, s)\Delta v^2 \end{aligned} \tag{68}$$

The C factors are called the **degapping parameters**; for HRC they have different values for each tap and tap side. Earlier detectors (Einstein and Rosat HRI) assumed C factors which were independent of coarse position.

The simplest choice of the degapping parameters is to take

$$\begin{aligned} C_{u1} &= C_{v1} = 1 \\ C_{u2} &= C_{v2} = 0, \end{aligned} \tag{69}$$

giving us **HRC raw tap coordinates**,

$$\begin{aligned} u_{raw} &= (u_{\text{coarse}} + u_{\text{fine}}) \\ v_{raw} &= (v_{\text{coarse}} + v_{\text{fine}}) \end{aligned} \tag{70}$$

These coordinates do not provide a continuous system over the detector, and an HRC image plotted in raw coordinates contains 'gaps'. With some choice of the degapping parameters, we obtain

a continuous (but not linear) system giving an image with no gaps. **HRC degapped coordinates** (u_{dg}, v_{dg}). Example values from Murray and Chappell (1989) of C used to give degapped coordinates are

$$\begin{aligned} C_{u1} &= C_{v1} &= 1.049 \\ C_{u2} &= C_{v2} &= 0.110, \end{aligned} \tag{71}$$

so

$$\begin{aligned} u_{dg} &= (u_{\rm coarse} + 1.049 u_{\rm fine} - 0.11 u_{\rm fine}|u_{\rm fine}|) \\ v_{dg} &= (v_{\rm coarse} + 1.049 v_{\rm fine} - 0.11 u_{\rm fine}|u_{\rm fine}|) \end{aligned} \tag{72}$$

The coefficients to be used for the HRC have not yet been determined.

5.2.3 HRC Chip Coordinates (HRC-1.1)

The HRC Telemetry Pixel Number System scales the taps by a pixel size $\Delta_t = 256$ to give

$$\begin{aligned} TELU &= (u + 0.5) * \Delta_t \\ TELV &= (v + 0.5) * \Delta_t, \end{aligned} \tag{73}$$

integer pixel numbers which start with pixel 0 (for a tap value of -0.5). This definition is corrected from the one in editions 4 and earlier of this memo.

For compatibility with other data archives, we add one to these engineering coordinates and then divide them up into individual chips to get HRC Chip Coordinates (AXAF-HRC-1.1)

$$CHIPX = (u - u_0) * \Delta_t + 0.5 = TELU - \Delta_t * (u_0 + 0.5) + 0.5 \tag{74}$$

$$CHIPY = (v - v_0) * \Delta_t + 0.5 = TELV - \Delta_t * (v_0 + 0.5) + 0.5 \tag{75}$$

$$\tag{76}$$

Note that $u_0 = -0.5$ always. v_0 = -0.5 for HRC-I; +0.5 for HRC-S1; 64.5 for HRC-S2; 126.5 for HRC-S3. This corresponds to HRC-S tap boundaries at 64.5 and 126.5. It returns us to a system in which the taps are numbered separately for each chip.

Table 11: HRC-S1 TELV, v and CHIPY

TELV	Coarse v, Fine v	CHIPY
0	0, -0.5	-255
16640	64, +0.5	16384

In this system, 1 pixel = 0.00643 mm = 0.13 arcsec. The size of one tap is 1.646mm. Now this coordinate system actually covers a larger area than the true possible coordinates. For instance,

v taps 0 and 1 for HRC-S1 are missing, so the lowest possible v coordinate in the telemetry for HRC-S is 1.5 (corresponding to tap 2 with fine position -0.5) but even this does not correspond to a valid detected event position. Nevertheless, we will define our logical coordinate system to cover the range of v coordinates starting at CHIPX, CHIPY = 0.5 (lower left corner of first pixel) which corresponds to HRC-S u, v = (-0.5, +0.5). Version 3.0 of this document defined chip coordinate system AXAF-HRC-1.0 which did not cover this full logical range and had a slightly different origin; the current system is denoted AXAF-HRC-1.1.

The center of HRC-S2 is then at $(u, v) = (7.5, 95.5)$ and the gaps between the MCPs are at v values of 62.96 to 64.12 and 124.88 to 126.04. In earlier work I arbitrarily set the chip boundaries at 63.0 and 126.0 so that each chip has a length of 63.0 taps, but on recommendation from M. Juda I have adjusted the chip sizes so that the true chip gaps fall on the logical chip boundaries.

Table 12: HRC electronically meaningful coordinate ranges

Chip	v_0	u	v	CHIPX	CHIPY	TELU	TELV
HRC-I	-0.5	0.0 to 63.0	0.0 to 63.0	0.5 to 16128.5	0.5 to 16128.5		
HRC-S1	0.5	0.0 to 15.0	1.5 to 64.5	128.5 to 3968.5	256.5 to 16384.5		
HRC-S2	64.5	0.0 to 15.0	64.5 to 126.5	128.5 to 3968.5	0.5 to 15872.5		
HRC-S3	126.5	0.0 to 15.0	126.5 to 190.5	128.5 to 3968.5	0.5 to 16384.5		

Now let's look at the boundaries on HRC-S and HRC-I more closely. We keep extra figures for self-consistency only assuming a tap scale of 1.6460 exactly, and measure positions starting at the physical position corresponding to chip pixel position 0.5 (bearing in mind this may be outside of the wire grid).

I used the following information on the HRC-S:

```
Tap size is 1.646 mm (M. Juda)
16384 pixels = 105.344 mm: logical chip size = tap size 1.646 mm x 64 taps
MCP physical size 100.000 mm x 27.000 mm from 'TOP MCP COORDINATES' drawing
Total logical length is 3 x 105.344 mm
Total physical length is 3 x 100.000 mm + 2 x gap size = 1.905 mm.
S2 Center is center of both total logical and total physical length.
Coating extends 94.5mm on outer MCPs and 16mm wide (M. Juda)

Post XRCF revision 1: (M Juda Oct 97)
S1 TELU range from 600 to 3496, TELV from 1190 to 16250 with
CsI limit at 1613.
S2 TELU from 600 to 3488, TELV from 16990 to 32261
S3 TELU from 600 to 3504, TELV from 32925 to 48110 with CsI
limit at 47650.

The coating strip is at TELU = 2660 (S1), 2670 (S2), 2670 (S3)
with the 'T' strip at TELV from 22780 to 27670.

More accurate post XRCF data: MCP edges at TELV = 16428, 17012, 32244, 32932.
```

This information leads to the following MCP layout :

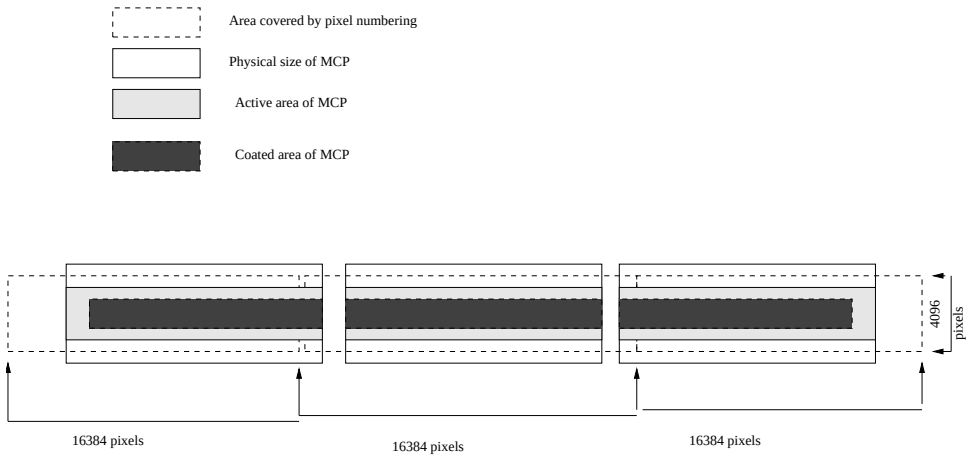

Figure 14: Relationship of HRC-S pixels to the physical instrument.

Table 13: HRC-S boundaries (Revised May 98)

Boundary	TELV	Tap v	Pos, mm	Seg No.	Y_{CPC}, mm	CHIPY, pix
S1 TELV = 0	0	-0.50	-1.646	1	-1.646	-255.5
S1 Logical Left Edge	256	0.50	0.000	1	0.000	0.5
S1 Electronic L Edge	512	1.50	3.292	1	3.292	256.5
S1 MCP Left Edge	873	2.91	3.970	1	3.970	617.5
S1 Active Left Edge	1190	4.15	6.005	1	6.005	934.5
S1 Coating edge	1613	5.80	8.724	1	8.724	1357.5
S1 Active Right Edge	16250	62.98	102.825	1	102.825	15994.5
S1 MCP Right Edge	16428	63.68	103.970	1	103.970	16172.5
S1 Logical Right Edge	16640	64.50	105.333	1	105.333	16384.5
S2 Logical Left Edge	16640	64.50	105.333	2	0.000	0.5
S2 Active Left Edge	16990	65.87	107.583	2	2.250	350.5
S2 MCP Left Edge	17012	65.95	107.724	2	2.390	372.5
S2 Center	24576	95.50	156.353	2	51.020	7936.5
S2 Measured center	24628	95.70	156.688	2	51.355	7988.5
S2 MCP Right Edge	32244	125.45	205.651	2	100.318	15604.5
S2 Active Right Edge	32261	125.52	205.760	2	100.427	15621.5
S2 Logical Right Edge	32512	126.50	207.374	2	102.041	15872.5
S3 Logical Left Edge	32512	126.50	207.374	3	0.000	0.5
S3 Active Left Edge	32925	128.11	210.029	3	2.655	413.5
S3 MCP Left Edge	32932	128.14	210.074	3	2.700	420.5
S3 Coating Edge	47650	185.63	304.696	3	97.322	15138.5
S3 Active Right Edge	48110	187.43	307.653	3	100.279	15598.5
S3 MCP Right Edge	48487	188.90	310.074	3	102.700	15975.5
S3 Electronic R Edge	48640	189.50	311.060	3	103.686	16128.5
S3 Logical Right Edge	48896	190.50	312.707	3	105.333	16384.5

Boundary	TELU	Tap u	X_{CPC}, mm	CHIPX, pix
MCP Edge		-1.620	-0.700	-286.2
TELU = 0	0	-0.500	0.000	0.5
Logical Edge		-0.500	0.000	0.5
Coating Edge		1.843	3.748	600.0
Center		7.500	12.800	2048.5
Strip Edge		9.930	16.688	2670.0
Coating Edge		13.172	21.875	3500.0

Logical Edge	15.500	25.600	4096.5
MCP Edge	15.937	26.300	4208.5

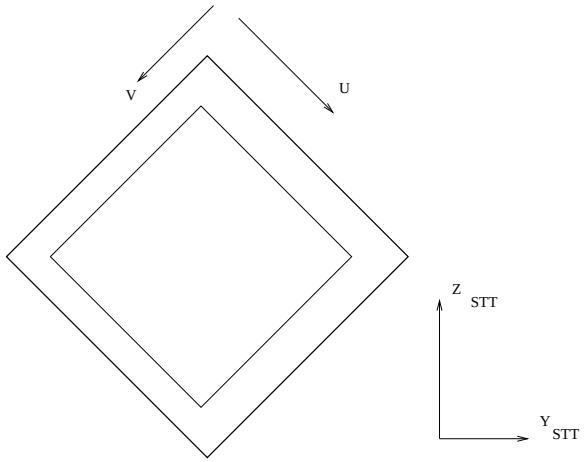

Figure 15: HRC-I pixel axes.

Table 14: HRC-I boundaries

Boundary	Tap u or v	X_{CPC} or Y_{CPC}, mm	CHIPX or CHIPY, pix
Logical Edge	-0.500	0.000	0.5
MCP Edge	1.123	2.672	416.1
Active Area	3.250	6.172	960.4
Coating Edge	4.161	7.672	1193.7
Center	31.500	52.672	8192.5
Coating Edge	58.839	97.672	15191.3
Active Area	59.750	99.172	15424.6
MCP Edge	61.877	102.672	15968.9
Logical Edge	63.500	105.344	16384.5

The CPC coordinates run from 0.0 to 26.33 (X_{CPC} for HRC-S) and from 0.0 to 105.3 (Y_{CPC} for HRC-S and both axes for HRC-I).

The active area of each microchannel plane is smaller, and the area coated with photocathode is smaller still. For HRC-I, the chip is 100 x 100 mm, with a 93 x 93 mm active area and a 90 x 90 mm coated area. For HRC-S, each chip is 100 x 27 mm, the active area is 100 x 20 mm, and the coated area is 94.5 x 16.0 mm. except for HRC-S2 where the coated area is 100 x 16 mm. Using these numbers, we derive the locations of the various areas in CPC (mm) and Chip (pixel)

coordinates listed above.

6 The SIM

6.1 Chip orientation summary tables

The following table gives the Euler rotation angles for the chips. The LSI to CPC transformation is more intuitive; the first angle ϕ indicates the tilt with respect to the LSI plane (with HRC-I having $\phi = 180$ to indicate being completely flipped over, another way of expressing the different handedness of its axes); and the third angle ψ indicates the rotation of the chip in the LSI Y,Z plane relative to chip I0.

Table 15: Euler angles in degrees for CPC to LSI coordinates

Chip	CPC to LSI	LSI to CPC
I0	Rot(180, 92.875, 177.129)	Rot(2.871, 92.875, 0.0)
I1	Rot(0, 92.872, 182.869)	Rot(-2.869, 92.872, 180.0)
I2	Rot(180, 87.125, 177.131)	Rot(2.869, 87.125, 0.0)
I3	Rot(0, 87.128, 182.871)	Rot(-2.871, 87.128, 180.0)
S0	Rot(90.0, 90.0, 179.088)	Rot(0.912, 90.0, 90.0)
S1	Rot(90.0, 90.0, 179.419)	Rot(0.581, 90.0, 90.0)
S2	Rot(90.0, 90.0, 179.751)	Rot(0.249, 90.0, 90.0)
S3	Rot(90.0, 90.0, 180.082)	Rot(-0.082, 90.0, 90.0)
S4	Rot(90.0, 90.0, 180.424)	Rot(-0.424, 90.0, 90.0)
S5	Rot(90.0, 90.0, 180.746)	Rot(-0.746, 90.0, 90.0)
HRC-I	Rot(-135.0, 90.0, 0.0)	Rot(180.0, 90.0, -45.0)
HRC-S1	Rot(0.0, 90.0, 181.426)	Rot(-1.426, 90.0, 180.0)
HRC-S2	Rot(0.0, 90.0, 180.0)	Rot(0.0, 90.0, 180.0)
HRC-S3	Rot(0.0, 90.0, 178.778)	Rot(1.222, 90.0, 180.0)

6.2 Relative positions of instruments

The location of the origins of the LSI system for each instrument are given in STT coordinates in the table below.

Table 16: Location of instrument origin on Translation Table

Values of $P_{STT}(S)$, i.e. offsets $S - \Sigma$	
ACIS origin	(0.0, 0.0, 237.4)
HRC-I origin	(0.15, 0.0, -126.6)
HRC-S origin	(0.10, 0.0, -250.1)

6.3 Aimpoints

Several named default aimpoints are defined for the various AXAF instruments. The table below gives the STF coordinates of the instrument table origin for each of these aimpoints. Most observations will use one of these default aimpoints, but in general the SIM can be moved in X and Z to any aimpoint.

Table 17: SIM position offsets for nominal focus positions

Values of $P_{STF}(\Sigma)$	
AI1 ACIS-I offset	(0.0, 0.0, -237.4)
AI2 ACIS-I offset	(0.0, 0.0, -233.9)
AS1 ACIS-S offset	(0.0, 0.0, -190.5)
HI1 HRC-I offset	(-0.15, 0.0, 126.6)
HS1 HRC-S offset	(-0.10, 0.0, 250.1)

7 The HRMA (flight)

7.1 HRMA nodal coordinates

The conversion from STF (instrument compartment) to MNC (HRMA nodal) coordinates requires knowledge of the focal length, which is 10065.0 mm.

$$\begin{pmatrix} X_{STF} \\ Y_{STF} \\ Z_{STF} \end{pmatrix} + \begin{pmatrix} f \\ 0 \\ 0 \end{pmatrix} = \begin{pmatrix} X_N \\ Y_N \\ Z_N \end{pmatrix} \tag{77}$$

In flight, the orientation of the SIM with respect to the HRMA is fixed. In the flight nominal configuration, one of the SIs has its nominal focal point at the telescope focus. However, the SIM can be moved so that the nominal focal point and the telescope focus do not coincide (general flight configuration).

7.2 Focal and Tangent plane systems

We define the following focal plane pixel systems, together with their usual purpose (although one may still use e.g. FP-2.0 with XRCF ACIS data, etc.). The coordinate systems are defined in terms of their physical pixel size at the nominal flight focal length f = 10065.0 mm. The corresponding angular sizes are also given, but the actual angular size will be different for XRCF/HRMA and XRCF/TMA data.

We define systems for the nicely rounded pixel sizes and for the accurate actual pixel sizes. We've decided to use the mean actual pixel sizes for the flight system. Thus, the size of an HRC-I

pixel at the nominal focal distance of 10065.0 mm is 0.132 arcseconds, so 0.132 arcseconds is defined as the FP-2.1 pixel size (even if the detector is moved well off focus). The HRC-S detector has a maximum linear extent of over 48500 pixels. When making sky coordinates for such a detector, we must define a square pixel plane (to allow for the roll angle). We choose a 65536 pixel sided plane, defined as FP-2.3. This plane has a total of 4.3 gigapixels, slightly more than can fit in a 4-byte signed integer. We therefore recommend not making full resolution full frame image files in this coordinate system.

Here are the current flight pixel systems:

System	Δ_{sp} (mm)	Δ_{s0} (arcsec)	t_x	t_y	FPX0, FPY0	Purpose
AXAF-FP-1.1	0.0240	0.492	+1	-1	4096.5	Flight ACIS, actual pixel
AXAF-FP-2.1	0.006429	0.132	+1	-1	16384.5	Flight HRC-I, actual pixel
AXAF-FP-2.3	0.006429	0.132	+1	-1	32768.5	Flight HRC-S

Here are the historically used pixel systems:

System	Δ_{sp} (mm)	Δ_{s0} (arcsec)	t_x	t_y	FPX0, FPY0	Purpose
AXAF-FP-1.0	0.0244	0.5	+1	-1	4096.5	Flight ACIS
AXAF-FP-1.1	0.0240	0.490	+1	-1	4096.5	Flight ACIS, actual pixel
AXAF-FP-2.0	0.0061	0.125	+1	-1	16384.5	Flight HRC
AXAF-FP-2.1	0.0064294	0.132	+1	-1	16384.5	Flight HRC-I, actual pixel
AXAF-FP-2.2	0.006429	0.132	+1	-1	23000.5	Flight HRC-S, test for long int constr
AXAF-FP-2.3	0.006429	0.132	+1	-1	25000.5	Flight HRC-S
AXAF-FP-3.0	0.0244	0.5	+1	+1	4096.5	XRCF ACIS, obsolete
AXAF-FP-3.1	0.0244	0.5	-1	-1	4096.5	XRCF ACIS
AXAF-FP-3.2	0.0240	0.483	-1	-1	4096.5	XRCF ACIS, actual pixel size
AXAF-FP-4.0	0.0061	0.125	+1	+1	16384.5	XRCF HRC, obsolete
AXAF-FP-4.1	0.0061	0.125	-1	-1	16384.5	XRCF HRC
AXAF-FP-4.2	0.0064294	0.129	-1	-1	16384.5	XRCF HRC, actual pixel size
AXAF-FP-4.3	0.0064294	0.129	-1	-1	32768.5 4196.5	XRCF HRC, new
AXAF-FP-5.1	0.00240	0.490	+1	+1	2048.5	ACIS-2C
AXAF-FP-5.2	0.0024	0.483	+1	+1	2048.5	ACIS-2C
AXAF-FP-6.1	0.00643	0.132	+1	+1	4096.5	HSI
AXAF-FP-6.2	0.00643	0.129	+1	+1	4096.5	HSI alternate

(The total image size should be 2*(FPX0-0.5)).

However, software should also support generic ASC-FP/TP coordinates with arbitrary pixel size

and sign choices.

7.2.1 Mosaicing XRCF images

We want to make mosaiced images which show the point spread function at different off axis angles over the whole field of view. The AXAF-FP-2.0 or -2.1 systems are therefore of interest. However, a single XRCF ACIS-2C image covers only a small part of the field. We don't want to make a 32768 square image when only a 4096 square part is used. As long as we stay in event list format, there is no storage problem, but in an image we should make only the minimal subset and store the location within the larger image as a WCS. The AXAF-FP-5.1,6.1 systems can be used for this purpose.

7.3 Angular systems

7.3.1 HRMA Left Handed Spherical Coordinates (AXAF-HSC-1.1)

This system is used to express off-axis angles. We define HRMA Spherical Coordinates (r, θ_H, ϕ_H) in terms of HRMA nodal Cartesian coordinates as follows:

$$\begin{pmatrix} X_N \\ Y_N \\ Z_N \end{pmatrix} = \begin{pmatrix} +r cos\theta_H \\ -r \sin\theta_H \cos\phi_H \\ r \sin\theta_H \sin\phi_H \end{pmatrix} \tag{78}$$

The inverse is

$$\begin{aligned} r &= \sqrt{X_N^2 + Y_N^2 + Z_N^2} \\ \theta_H &= \cos^{-1}(X_N/r) \\ \phi_H &= \arg(-Y_N, Z_N) \end{aligned} \tag{79}$$

This coordinate system is also used for input to the XRCF Test Database; it is a LEFT HANDED coordinate system. The XRCF test database immediately converts these to pitch and yaw. The north pole of this system is the center of the forward aperture of the HRMA A0; θ_H measures the off-axis angle of the incoming ray and ϕ_H measures its azimuth in the Y_N, Z_N plane such that for an observer at XRCF standing by the SI and looking at the XSS, $\phi_H = 0$ is to the left and $\phi_H = \pi/2$ is vertically downwards.

Then the forward aperture of the HRMA, A0, has HRMA nodal coordinates $(a, 0, 0)$ and HSC coordinates $(a, 0, 0)$. The focal point F of the HRMA has HRMA nodal coordinates $(-f, 0, 0)$ and HSC coordinates $(f, \pi, 0)$.

The HSC-1.1 system actually makes most sense when looking in the sky plane. Consider a source in the sky when roll angle is zero:

- *The FPX, FPY and X, Y axes are aligned.*

- *RA, Dec are parallel to -X, +Y. (since RA increases toward the left looking at the sky).*
- *The +X, +Y axes are parallel to -SCY, +SCZ. A photon from larger Dec and smaller RA than the field center comes from the +X, +Y direction. It enters the telescope from -SCY, +SCZ, and therefore has HSC coordinate azimuth between +0 and +90 deg. Thus, the HSC azimuth is just the conventional plane polar coordinate angle in the +FPX, +FPY tangent plane coordinate system.*
- *After passing through the (ideal) mirror origin, the photon leaves from +SCY, -SCZ and lands at +LSI Y, -LSI Z. (The HSC coordinates of the outgoing photon have azimuth between 180 and 270, and off axis angle between 90 and 270, but this is not normally of interest.)*

7.3.2 HRMA Right Handed Spherical Coordinates (AXAF-HSC-1.2)

To satisfy my desire for using left handed systems as little as possible, I defined HSC-1.2 to be the same as HSC-1.1 except that the azimuth increases in the opposite direction: $\phi_{HR} = 0$ is to the left and $\phi_{HR} = \pi/2$ is vertically upwards. *This system has not been used and is now deprecated.*

$$\begin{pmatrix} X_N \\ Y_N \\ Z_N \end{pmatrix} = \begin{pmatrix} rcos\theta_{HR} \\ -r\sin\theta_{HR}\cos\phi_{HR} \\ -r\sin\theta_{HR}\sin\phi_{HR} \end{pmatrix} \tag{80}$$

The inverse is

$$\begin{aligned} r &= \sqrt{X_N^2 + Y_N^2 + Z_N^2} \\ \theta_{HR} &= \cos^{-1}(X_N/r) = \theta_H \\ \phi_{HR} &= \arg(-Y_N, -Z_N) = -\phi_H \end{aligned} \tag{81}$$

7.3.3 HRMA rotation coordinates (Pitch and Yaw) (AXAF-HSC-3.0)

A third choice of pole is the $+Y_N$ axis, whose latitude-like coordinates α_z is called **yaw**, and whose azimuthal coordinate α_y is called **pitch**. The mapping between pitch and yaw coordinates and HRMA coordinates is

$$\begin{pmatrix} X_N \\ Y_N \\ Z_N \end{pmatrix} = \begin{pmatrix} +r\cos\alpha_z\cos\alpha_y \\ +r\sin\alpha_z \\ -r\cos\alpha_z\sin\alpha_y \end{pmatrix} \tag{82}$$

or

$$\begin{aligned} \alpha_z &= \sin^{-1}(Y_N/r) \\ \alpha_y &= \arg(X_N, -Z_N) \end{aligned} \tag{83}$$

The rotation matrix from HSC-1.2 right-handed spherical coords is

$$\mathrm{R(HSC\text{-}1.2,HSC\text{-}3.0)} = \mathrm{Rot}(\pi, \pi/2, \pi). \tag{84}$$

The motivation for this coordinate system is its relationship to the commanded pitch and yaw of the HRMA at XRCF. We call the pitch and yaw coordinates of the XSS $\alpha_y(XSS) = \alpha_{y0}$ and $\alpha_z(XSS) = \alpha_{z0}$. To put the XSS at these coordinates, the HRMA must be yawed α_{z0} to the left and its aperture pitched α_{y0} downward.

7.3.4 HRMA Source coordinates (AXAF-HSC-2.1)

The HRMA Source Coordinate system (r, az, el) is a pseudo RA, Dec system that gives the 'sky' position of the source as seen by the HRMA. Unlike HRMA spherical coordinates, they have a pole at $-Z_N$ rather than X_N. The relationship between Source coordinates and HRMA nodal coordinates is:

$$\begin{pmatrix} X_N \\ Y_N \\ Z_N \end{pmatrix} = \begin{pmatrix} +r\cos\mathrm{el}\cos\mathrm{az} \\ -r\cos\mathrm{el}\sin\mathrm{az} \\ -r\sin\mathrm{el} \end{pmatrix} \tag{85}$$

Coordinates az =0, el = 0 refer to a source on the HRMA axis (center of the field of view); positive el gives a source above the HRMA axis (top of the field of view), while positive az gives a source to the left of the center of the field of view. (HSC-2.0 had az going the other way, creating a left-hand system). The inverse function is

$$\begin{aligned} \mathrm{el} &= \sin^{-1}(-Z_N/r) \\ \mathrm{az} &= \arg(X_N, -Y_N) \end{aligned} \tag{86}$$

The rotation matrices from the other HRMA angular systems are

$$\mathrm{R(HSC\text{-}1.2,HSC\text{-}2.1)} = \mathrm{Rot}(\pi/2, \pi/2, \pi); \quad \mathrm{R(HSC\text{-}3.0,HSC\text{-}2.1)} = \mathrm{Rot}(\pi/2, \pi/2, 3\pi/2). \tag{87}$$

8 HETG and LETG

The Grating Node is on the optical axis at a distance R from the focus, where R is the diameter of the Rowland Circle. The nominal Rowland Circle diameter is quoted as 8650.0 mm [1], Appendix A, p. 11; 8633.69 mm [1], Drawing 301331, Sheet 3; and 8636.00 mm [3]. I will adopt the value from the drawing, i.e. 8633.69mm. (However View F on the same drawing shows the Rowland circle intercepting the X axis at $X_A = 372.116$ corresponding to R = 8643.11 mm. This is an error caused by confusing H0 and H1 when measuring the location of the OTG origin.)

The MNC coordinates of the Grating Node ***G0*** in flight are

$$\begin{pmatrix} X_N(G0) \\ Y_N(G0) \\ Z_N(G0) \end{pmatrix} = \begin{pmatrix} -1431.81 \\ 0 \\ 0 \end{pmatrix} \tag{88}$$

The exact value is different at XRCF. We use the same physical pixel size as for the detector systems, which correspond to somewhat different angular sizes than the imaging case because we are measuring angles from G rather than H0. However, in the case of ACIS, we hope to get extra resolution by using the sub-pixel dither of the detector relative to the sky coordinate zero order position. So, in the GDP-1.1 system we have chosen the GDP pixel size for ACIS and HRC to be the same 6 micron value. (In an earlier version of this memo, the GDP-1.0 system was described with 24 micron ACIS GDP pixel sizes. That system was never implemented.)

What is the extent of the GDP coordinate system? In the case of HRC-S, our worst case is a zero order at an extreme end of the 3-chip array. In that case, you could be as many as 49152 pixels down the dispersion coordinate. This is such a pathological case that we have decided not to build our definitions around it. A normal case would be a zero order in the center, with dispersion coordinates up to plus or minus 25000 pixels or so. As a compromise to support most off axis cases, we adopt pixels running from 1 to 65536 in the dispersion direction, giving 32768 pixels on either side of zero order. In the cross dispersion direction, with HRC-I as the detector, we might have photons up to 16384 pixels from the zero order in principle, and 8192 even if the source is centered in the detector. For ACIS, the extreme range is 32678 super-resolved pixels in the dispersion direction and 24800 pixels in the cross dispersion direction. For both ACIS and HRC, the GDP-1.1 system is sized to be 65536 pixels in the dispersion direction and 32678 pixels in the cross dispersion direction, with the zero order position at (32768.5, 16384.5). However, we recommend that in normal use the 32768 x 4096 subarray extending from (16384,14336) to (49152,18432) be used. This subarray is defined as AXAF-GDP-1.2; it has the same pixel size as GDP-1.1.

Table 20: GDC pixel image centers

Instrument	System	GDX0, GDY0	Image size
ACIS,HRC	GDP-1.1	32768.5, 16384.5	65536 x 32768
ACIS,HRC	GDP-1.2	16384.5, 2048.5	32768 x 4096

Table 21: GDP Pixel Sizes (assuming flight Rowland radius)

Instrument	System	Size at Focal Plane Δ_p, Δ_{gp} (mm)	Angular Size $\Delta_g s$ (arcsec)
ACIS	GDP	0.006430	0.154

HRC	GDP	0.006430	0.154

The average grating periods for the three gratings are given in the table below.

Table 22: Grating properties

Instrument	P	α_G (deg)
HETG	2000.0$\AA$	5.0
METG	4000.0$\AA$	-5.0
LETG	9921.0$\AA$	+0.0

9 XRCF

9.1 XRCF coordinates

For much of XRCF, the HRMA sits aligned with the Facility Optical Axis in its 'rest' position, but it can be tilted in two axes. We therefore need to distinguish between facility (XRCF) coordinates and mirror (MNC) coordinates.

In the XRCF, we have the HRMA mounted on two axes - it can change its yaw (azimuth) and pitch (elevation), or equivalently the polar angle and polar azimuth. The instrument (SI) is mounted on either the FAM (Five Axis Mount) or the HXDS (HRMA X-ray Detection System). In the **default configuration** C0, the HRMA axis and the SI are aligned with the FOA (Facility Optical Axis) and the SI nominal focus S is located at the actual focus F. The X-ray Source System (XSS) is fixed in the XRCF frame and lies on the positive X_{XRCF} axis (see below).

The origin of XRCF coordinates is at the HRMA CAP (H1).

10 ACIS-2C

The ACIS-2C instrument is used for ground calibration at XRCF. The two chips are similar to the flight ACIS chips, and will frequently be used in Fast Window mode.

Table 23: Tiled Detector Plane systems - ACIS-2C

System	Size	X Center, Y Center	Use
AXAF-ACIS-2.4	4096 x 2048	(2048.5, 1024.5)	XRCF ACIS-2C

Table 24: Parameters of Tiled Detector Coordinate definitions

Tiled System	Chip	θ_i	Δ_i	$X0_i$	$Y0_i$	H_i
AXAF-ACIS-2.4	ACIS-C0	0	1	304.0	512.0	1
AXAF-ACIS-2.4	ACIS-C1	0	1	1536.0	512.0	1

The ACIS-2C chip centers are separated by approximately 63.0 mm.

Table 25: ACIS-2C chip corner locations in ACIS-2C LSI coordinates

Chip	Corner	CPC coords	ACIS-2C LSI coords
C0	LL	(0.0, 0.0, 0.0)	(0.000, 47.57, 11.10)
	LR	(24.58, 0.0, 0.0)	(0.000, 22.99, 11.10)
	UR	(24.58, 24.58, 0.0)	(0.000, 22.99, -13.48)
	UL	(0.0, 24.58, 0.0)	(0.000, 47.57, -13.48)
C1	LL	(0.0, 0.0, 0.0)	(-0.342, -15.18, 10.45)
	LR	(24.58, 0.0, 0.0)	(-0.342, -39.76, 10.45)
	UR	(24.58, 24.58, 0.0)	(-0.342, -39.76, -14.13)
	UL	(0.0, 24.58, 0.0)	(-0.342, -15.18, -14.13)

11 HSI

Just as ACIS-2C is like a small ACIS, HSI is like a small HRC.

HSI has 16 taps on its side and an area of 18 mm.

Table 26: HSI boundaries

Boundary	Tap u or v	X_{CPC} or Y_{CPC}, mm	CHIPX or CHIPY, pix
Logical Edge	-0.500	0.000	0.5
MCP Edge	2.032	4.168	648.7
Active Area	?		
Coating Edge	?		
Center	7.500	13.168	2048.5
Coating Edge	?		
Active Area	?		
MCP Edge	13.970	22.168	3448.3
Logical Edge	15.500	26.336	4096.5

Table 27: Parameters of Tiled Detector Coordinate definitions

Tiled System	Chip	θ_i	Δ_i	$X0_i$	$Y0_i$	H_i
AXAF-HSI-2.3	HSI	0	1	0.0	0.0	1

Table 28: HSI chip corner locations in HSI LSI coordinates

Chip	Corner	CPC coords	HSI LSI coords
HSI	LL	(0.0, 0.0, 0.0)	(0.000, -13.17, -13.17)
	LR	(26.34, 0.0, 0.0)	(0.000, 13.17, -13.17)
	UR	(26.34, 26.34, 0.0)	(0.000, 13.17, 13.17)
	UL	(0.0, 26.34, 0.0)	(0.000, -13.17, 13.17)

11.1 Instrument origins

Table 29: Location of instrument origin on Translation Table, XRCF

Values of $P_{STT}(S)$, i.e. offsets $S - \Sigma$	
ACIS origin	(0.0, -5.35, 67.20)
HRC-I origin	(0.0, 0.0, 517.988)
HRC-S origin	(0.0, 0.0, 637.480)
HSI origin	(0.0, 0.0, 0.0)
ACIS-2C origin	(0.0, 0.0, 65.002) (Phase F)
ACIS-2C origin	(0.0, -4.33 133.310) (Phase G)

In addition, the raw FAM values must be adjusted by (87.92, 12.94, 7.55) to get FAM coordinates relative to the DFC origin.

11.2 HRMA motion

In the **nominal configuration** CN, the HRMA is tilted but the SI is moved so that its normal X_{LSI} axis remains coincident with the HRMA optical axis X_{XRCF}. In the most general configuration the HRMA and SI are both moved relative to the XRCF but the X_{LSI} axis is not made to coincide with the X_{XRCF} axis.

WARNING: The terms '**on-axis**' and '**off-axis angle**' are correctly used to refer to an angle relative to the optical axis of the HRMA. However, at XRCF they are sometimes used to mean an angle relative to the Facility Optical Axis, which could lead to confusion. I will always use the concept of on and off axis to refer to the HRMA optical axis.

The Y_{LSI}, Z_{LSI} plane contains the science instrument, which returns coordinate values of events measured in detector pixels CHIPX, CHIPY from each of several discrete planar 'chips' (or MCPs in the case of HRC). In data analysis we consider two complementary problems:

- The forward case: Given an XRCF configuration, at which chip CHIP_ID and chip pixel CHIPX, CHIPY will the XSS photons fall? In other words, where do we expect the image to be?
- The inverse case: Given a photon landing on chip CHIP_ID and chip pixel CHIPX, CHIPY, from which direction (off-axis angle and azimuth) did the incoming photon approach the HRMA?

11.2.1 XRCF to MNC transformation

We assume that the roation is around the point $O_{MNC} = (0,\ 0,\ 0)$ in MNC coordinates, or (XH, 0, 0) in XRCF coordinates, where $XH = 9.42$.

In terms of the pitch and yaw, the transformation between XRCF and MNC coordinates is given by the translation vector $(X_N(H1), 0, 0) = (XH, 0, 0)$, and the Euler rotation matrix

$$R(XRCF, MNC) = Rot(\alpha_z, \pi + \alpha_y, \pi) \tag{89}$$

or explicitly

$$\begin{aligned} X_N &= (X_{XRCF} - XH)\cos\alpha_z \cos\alpha_y + Y_{XRCF}\sin\alpha_z \cos\alpha_y - Z_{XRCF}\sin\alpha_y \\ Y_N &= (X_{XRCF} - XH)\sin\alpha_z - Y_{XRCF}\cos\alpha_z \\ Z_N &= -(X_{XRCF} - XH)\cos\alpha_z \sin\alpha_y - Y_{XRCF}\sin\alpha_z \sin\alpha_y - Z_{XRCF}\cos\alpha_y \end{aligned} \tag{90}$$

and the inverse

$$\begin{aligned} X_{XRCF} &= XH + X_N \cos\alpha_z \cos\alpha_y + Y_N \sin\alpha_z - Z_N \cos\alpha_z \sin\alpha_y \\ Y_{XRCF} &= X_N \sin\alpha_z \cos\alpha_y - Y_N \cos\alpha_z - Z_N \sin\alpha_z \sin\alpha_y \\ Z_{XRCF} &= -X_N \sin\alpha_y - Z_N \cos\alpha_y \end{aligned} \tag{91}$$

Note that for zero pitch and yaw,

$$\begin{aligned} X_N &= (X_{XRCF} - XH) \\ Y_N &= -Y_{XRCF} \\ Z_N &= -Z_{XRCF} \end{aligned} \tag{92}$$

reflecting the fact that the mirror is installed upside down at the XRCF.

So in particular if the focal point $P_N(F) = (-f, 0, 0)$ then

$$P_{XRCF}(F) = (XH - f\cos\alpha_z \cos\alpha_y, -f\sin\alpha_z \cos\alpha_y, f\sin\alpha_y) \tag{93}$$

For some reason the Ball SER approximates this as

$$P_X(F) \sim (-f\cos\sqrt{(\alpha_z^2+\alpha_y^2)}, -f\sin\alpha_z, f\sin\alpha_y) \tag{94}$$

which is OK for small α_y,α_z.

The XSS is at HRMA nodal coordinates

$$\begin{pmatrix} X_N(XSS) \\ Y_N(XSS) \\ Z_N(XSS) \end{pmatrix} = \begin{pmatrix} +LS\cos\alpha_z\cos\alpha_y \\ +LS\sin\alpha_z \\ -LS\cos\alpha_z\sin\alpha_y) \end{pmatrix} \tag{95}$$

11.3 HXDS Motion

The HXDS stage moves in XRCF X, Y and Z. For a tilted mirror, one must convert from XRCF X, Y and Z to MNC X, Y and Z to obtain the STF to MNC translation-rotation matrix.

11.4 FAM Motion

Treatment of the FAM is complicated by the fact that the FAM axes are inverted with respect to the mirror axes.

The FAM rotates and translates the origin of STF coords, O_{STF}, relative to the facility optical axis, O_{XRCF}. The three translational axes of the FAM define a (moving) FAM coordinate system with origin at O_{STF}. Move the FAM to the FOA so that the STF and FC origins coincide; then the FAM coordinate system is coincident with a (fixed) DFC (Default FAM Coordinate) system which is almost aligned with the XRCF axes. We record the transformation from DFC to XRCF axes as:

$$P(XRCF) = R(DFC, XRCF)P(DFC)$$

where the matrix is a misalignment matrix close to unity. Let the FAM position readouts at O_{XRCF} be F0. Now move the FAM to an arbitrary position with FAM readouts F. Then the DFC coordinates of the STF origin are

$$O_{STF}(DFC) = F - F0$$

and the DFC coordinates of a position with FAM coords P(FAM) are

$$P(DFC) = O_{STF}(DFC) + R(DFC, FAM)P(FAM).$$

Now the instrument is mounted on the LASSZ (a simulator for the SIM translation table). Let the LASSZ reading be L, and the LASSZ reading when $O_{STT} = O_{STF}$ be L0. The sign of LASSZ is such that L increases with XRCF +Z, FAM +Z, or SC -Z, STF -Z. A point with LSI coordinates P(LSI) has FAM coordinates

$$P(FAM) = -P(LSI) - O_{LSI}(STT) + L - L0$$

So from this we can go from P(LSI) to P(FAM) and hence P(XRCF).

Let's consider a FAM move with the HRMA held constant. At the start, the beam is at chip coords CX0, CY0, and the focal plane coordinates of CX0, CY0 are the central values FX0, FY0. Move the FAM to larger Y,Z FAM readouts. The FAM moves to larger +Y, +Z in XRCF coordinates; the beam will then move to smaller chip coords CX, CY (the detector moved up and to the right, so the beam, which stays put, lands nearer to the lower left of the detector). of course the beam's FP coords remain the same. The FP coords of the old chip position CX0, CY0 have moved to larger values of FX0, FY0 (in the default XRCF focal plane system with signs -1,-1).

The pixlib routine pix_setup_mirror gets its arguments in FAM coordinates. The mirror angles are also chosen wrt XRCF signs. Specifically, FAM angles of all zero result in an STF to DFC transformation which inverts STF relative to DFC.

The HXDS stage axis misalignment is from a 1996 Dec 27 memo of Ian Evans.

Table 30: Assumed Misalignments

Stage	Angles (arcmin)
HXDS	(0.0, 1.6, -16.4)
FAM	(0.0, 0.0, 0.0)

11.5 FAM Motion, old copy

The FAM data file returns relative XRCF coordinates which we will designate as $P_{FAM}(XRCF) = X_{FAM}, Y_{FAM}, Z_{FAM}$ and absolute XRCF orientations $\theta_x, \theta_y, \theta_z$. We need to convert this to an STF-MNC translation-rotation matrix. Let us assume we have converted the FAM variables to units of mm and radians. Then from Part 1 of this memo, we need to find the parameters of

$$P(MNC) = O_{STF}(MNC) + R(STF, MNC)P(STF). \tag{96}$$

These are

$$O_{STF}(MNC) = R(XRCF, MNC)(O_{STF}(XRCF) - O_{MNC}(XRCF)) \tag{97}$$

and

$$R(STF, MNC) = R(XRCF, MNC)R(FAM, XRCF)R(STF, SIC) \tag{98}$$

(The earlier versions of this memo used a misalignment matrix to allow for FAM axis misalignment with the XRCF. In the present version it is assumed that this misalignment has been taken out by Ball in the data coming from the FAM).

Now

$$O_{STF}(XRCF) = O_{FAM}(XRCF) + dO_{FAM}(XRCF) + P_{FAM}(XRCF) \tag{99}$$

where O_{FAM} is the XRCF focus at XRCF coordinates (XH-f,0,0) and dO is the offset of the FAM coordinate origin relative to that point. The trouble is that we don't reliably know dO_{FAM} and it

can change every time the FAM is switched off and on. It must be derived from measurements of the beam centroid. The FAM rotation matrix is

$$R(FAM, XRCF) = Rot(3\pi/2, \theta_x, \pi/2)Rot(\theta_y, \theta_z, 0) \tag{100}$$

12 AXAF Spacecraft

In this section I describe the geometry of the AXAF spacecraft and other coordinate systems used in the project.

- The primary positional reference is the HRMA Central Aperture Plate (CAP) reference point, which I will designate $\boldsymbol{H1}$. This is the origin of AXAF Project HRMA coordinates. It is offset from our data analysis reference point, the nominal optical node $\boldsymbol{H0}$. $\boldsymbol{H1}$ is a physical datum which can be surveyed, while $\boldsymbol{H0}$ is a theoretical point which must be modelled. It is the nominal 'thin lens' position from which we measure off-axis angles at the focal plane - it's where the photons 'appear to come from'. If this were exactly true, we'd have a constant plate scale, but actually the effective nodal point depends both on energy and off-axis angle. Nevertheless, we can adopt a conventional nodal point and make astrometric position corrections as a function of position and energy, relative to the positions derived using that conventional nodal point.
- Another reference point is $\boldsymbol{G1}$, the origin of project OTG coordinates. The analogous data analysis reference point is $\boldsymbol{G0}$, the nominal grating node.
- Reference point $\boldsymbol{X1}$ marks the origin of Spacecraft Coordinates, a fictitious point out in space beyond the SIM.
- Reference point $\boldsymbol{F}$ is the flight focal position.
- $\boldsymbol{A0}$, the center of the aperture in the spacecraft-to-IUS interface plane.
- $\boldsymbol{A1}$, the center of the aperture at the front edge of the paraboloids (which is the origin of the ray trace system).

12.1 Project coordinate systems

12.1.1 Spacecraft coordinates (SC-1.0)

The Spacecraft (Observatory) coordinate system X_A, Y_A, Z_A (SC/TS ICD 4 Nov 1992, 3.2.1.1.1) is as follows: [1],[2] The X axis is parallel to the HRMA centerline; the aperture is toward positive X, while the SIM is at lower values of X. The Y and Z axes are in the plane of the SIM, such that

the ACIS radiator is toward positive Z and the Y axes completes an X, Y, Z right handed set. The coordinates are also called SCX, SCY, SCZ when we want to refer to a spacecraft coordinate system in general rather than AXAF in particular. (X_A, Y_A, Z_A) are measured in 'inches', which is a unit of length defined to be exactly 0.02540m. The center of the aperture in the AXAF/IUS interface plane is defined to have coordinates (500, 0, 0). The spacecraft trunnion plane has SCZ=14. The coordinates of the HRMA nodal point ***H0*** in SC coordinates are $(X_A(H0), 0, 0)$ where the value of $X_A(H0)$ is 428.116. The focus is at $(31.836, 0.0, 0.0)$.

12.1.2 HRMA coordinates (HRMA-2.0)

The project has defined Cartesian coordinates (X_H, Y_H, Z_H) fixed in the HRMA cap midplane, which are called **HRMA coordinates**. The origin of HRMA coordinates ***H1*** is at the HRMA CAP reference point. The HRMA X_H axis is along the HRMA optical axis, and positive X is toward the entrance aperture. Units of HRMA coordinates shall be mm.

The Spacecraft and HRMA coordinate systems are the fundamental ones for hardware alignment, but for data analysis of observations it's easier to use the HRMA nodal point ***H0*** as origin. This point is calculated to be offset by 17.577 mm from the HRMA CAP midplane (the value may change). The HRMA mirror nodal coordinate (MNC) system is (X_N, Y_N, Z_N), where

$$\begin{pmatrix} X_N \\ Y_N \\ Z_N \end{pmatrix} = \begin{pmatrix} X_H - X_H(H0) \\ Y_H \\ Z_H \end{pmatrix} \tag{101}$$

The finite conjugate focus is at HRMA nodal coordinates (-10258.3, 0.0, 0.0). (IF1-20 Obs/SI ICD). Note that

$$\begin{pmatrix} X_N \\ Y_N \\ Z_N \end{pmatrix} = \begin{pmatrix} (SCX - SCX(H0)) * 25.4 \\ SCY * 25.4 \\ SCZ * 25.4 \end{pmatrix} \tag{102}$$

where SCX(H0) (or $X_A(H0)$) is +428.116.

In the following table are listed reference points for various parts of the spacecraft. For XRCF, I give XRCF coordinates in inches for easy comparison with the drawings, although elsewhere in this document XRCF coordinates are measured in mm.

Table 31: Interesting points in spacecraft and HRMA nodal coordinates

		Flight		
Point	Description	(X_A, Y_A, Z_A)	(X_N, Y_N, Z_N)	Ref
X1	SC coordinate origin	(0.0, 0.0, 0.0)	(-10874.146, 0.0, 0.0)	
F	Flight Focus	(31.836, 0.0, 0.0)	(-10065.500, 0.0, 0.0)	[1],p.9

	Translation Table surface	(55.836, 0.0, 0.0)	(-9455.91, 0.0, 0.0)	[1],p.17
	ISIM to OBA interface	(60.336, 0.0, 0.0)	(-9341.6, 0.0, 0.0)	[1],p.9
G1	OTG Origin	(369.245, 0.0, 0.0)	(-1495.3, 0.0, 0.0)	[1],dr. 301331/3
	OTG Datum	(370.915, 0.0, 0.0)	(-1452.9, 0.0, 0.0)	[1],dr. 301331/3
G0	OTG Node	(371.745, 0.0, 0.0)	(-1431.810, 0.0, 0.0)	[1], dr.301331/3
H1	HRMA CAP reference point	(427.745, 0.0, 0.0)	(-9.42, 0.0, 0.0)	[1], dr.301331/3
H0	HRMA nodal point	(428.116, 0.0, 0.0)	(0.0, 0.0, 0.0)	[1], dr.30133/31
A1	Front end of paraboloids	(462.474, 0.0, 0.0)	(872.692, 0.0, 0.0)	
A0	Aperture center in IUS I/F plane	(500.0, 0.0, 0.0)	(1825.85, 0.0, 0.0)	[2],[1],p.9

XRCF				
Point	Description	X_{XRCF} (in)	(X_N, Y_N, Z_N)	Ref
F0	XRCF Default Focus	-403.5	(-10258.3, 0.0, 0.0)	[1], dr. 301331/5
G1	OTG Origin at XRCF	-60.613	(-1549.0, 0.0, 0.0)	[1]
	OTG Datum at XRCF	-58.943	(-1506.57, 0.0, 0.0)	[1]
G0	OTG Node at XRCF	-58.113	(-1485.49, 0.0, 0.0)	[1]
H1	HRMA CAP reference point	0.0	(-9.42, 0.0, 0.0)	
H0	HRMA nodal point	-0.37	(0.0, 0.0, 0.0)	

Table 32: Geometrical layout of mirrors and detectors:
Value of MNC X Coord X_N

Point	Description	TMA/TOGA	HRMA (XRCF)	HRMA (Flight)
F	On Axis Focus	-6068.61	-10258.3	-10065.50
G0	On Axis Rowland Circle	-702.06	-1485.49	-1431.81
	Shutter Plane	-546.06	Unknown	None
	Hyperbola back	-400.88	Unknown	Unknown
	Hyperbola front	-40.43	Unknown	Unknown
H0	Mirror Node	0.0	0.0	0.0
	Parabola back	40.42	Unknown	Unknown
A1	Front end of mirror	400.94	872.692	872.692

Table 33: Mirror radii, mm

Description	TMA/TOGA	Shell 1	Shell 3	Shell 4	Shell 6
Gratings	187.7?				

Hyperbola back	199.87773				
Hyperbola front	209.07069				
Midplane	210.00000				
Parabola back	210.30940				
Parabola front	213.33744	1200	960	850	620

12.2 Project Coordinate Systems

There are a plethora of existing coordinate systems in use describing positions relative to the HRMA mirror. They are used in the assembly and alignment of the hardware but they will not be used in the kind of data analysis I am concentrating on in this memo. They are presented for reference.

12.2.1 Orbiter coordinate system

The Space Shuttle Orbiter coordinate system [1] is used to locate the spacecraft within the Orbiter payload bay during the launch phase. It is measured in inches with the $+X_O$ axis downwards at launch (i.e. toward orbiter aft end), the $+Y_O$ axis to starboard, and the $+Z_O$ axis toward the top side (tail side) of the orbiter (i.e. upwards at landing). During launch, the origin of spacecraft coordinates is at orbiter coordinates

$$\begin{pmatrix} X_O \\ Y_O \\ Z_O \end{pmatrix} = \begin{pmatrix} 596.0 \\ 0.0 \\ 400.0 \end{pmatrix} \tag{103}$$

The relation between Orbiter and Spacecraft coordinates is

$$\begin{pmatrix} X_A \\ Y_A \\ Z_A \end{pmatrix} = \begin{pmatrix} X_O - 596.0 \\ Y_O \\ Z_O - 400.0 \end{pmatrix} \tag{104}$$

12.2.2 Payload coordinate system

The Space Shuttle payload coordinate system [1] is fixed with respect to the payload, probably. It is measured in inches. In the stowed position, payload and Orbiter coordinates are parallel, and related by

$$\begin{pmatrix} X_P \\ Y_P \\ Z_P \end{pmatrix} = \begin{pmatrix} X_O - 596.0 \\ Y_O \\ Z_O - 200.0 \end{pmatrix} = \begin{pmatrix} X_A \\ Y_A \\ Z_A + 200.0 \end{pmatrix} \tag{105}$$

(reference [1].)

12.2.3 The Telescope Ensemble Coordinate System

The document EQ7-002 Rev D, [4] describing the HRMA, defines the Telescope Ensemble Coordinate System (X_T, Y_T, Z_T) with somewhat different axis choice (+Z is the optical axis) and with origin at the focus. Presumably this is the on-orbit, zero-g focus f0, but the document doesn't say. The document IF1-20 OBS/SI ICD [1] defines the Telescope Coordinate System (X_T, Y_T, Z_T) to be identical with spacecraft coordinates.

12.2.4 Optical Bench Assembly system

The OBA system [2] is

$$\begin{pmatrix} X_{OBA} \\ Y_{OBA} \\ Z_{OBA} \end{pmatrix} = \begin{pmatrix} X_{FP} - 28.5 \\ Y_{FP} \\ Z_{FP} \end{pmatrix} = \begin{pmatrix} X_A - 60.336 \\ Y_A \\ Z_A \end{pmatrix} \tag{106}$$

(TRW AXAF I system alignment plan). I won't discuss it further.

12.2.5 OTG Coordinates (OTG-2.0)

The OTG coordinates system (X_G, Y_G, Z_G) has X_G parallel to X_H and Y_G, Z_G parallel to Y_A, Z_A $X_G = 0$ is the side of the OTG closest to the focal plane. This system (AXAF-OTG-2.0) is offset by 2.50 in (63.5mm) relative to the Grating Nodal system (AXAF-OTG-1.0) of interest for data analysis.

The HETG dispersion direction is rotated 5 deg counterclockwise from Y_A viewed from $X_A = 0$. METG is rotated the same amount clockwise. The inner and outer radii of the OTG are 234.95 and 558.80 mm.

12.2.6 Project FPSI Coordinate System

The Focal Plane Science Instruments coordinate system (X_F, Y_F, Z_F) is essentially identical to the LSI system defined in this document. However, the SE30 [2] definition specifies the origin as the 'desired aim point', while my LSI definition specifically selects a single nominal aim point for each instrument.

12.2.7 SIM and ISIM coordinates

ISIM coordinates are defined in the OBS/SI ICD [1] with their origin at spacecraft coordinates (31.836, 0.0, 0.0) near the focus (and thus defined only while the spacecraft is assembled); SIM coordinates are defined in the System Alignment Plan D17388, with their origin at the SIM/OBA interface. Both are usually measured in inches. I recommend use of the more generally defined data

analysis coordinate systems FP (fixed wrt the HRMA) and STF (fixed wrt the SIM) defined below. SIM and OBA coordinates are identical after assembly.

$$(X_{ISIM}, Y_{ISIM}, Z_{ISIM}) = (X_A, Y_A, Z_A) - \begin{pmatrix} 31.836 \\ 0 \\ 0 \end{pmatrix}$$

and

$$(X_{SIM}, Y_{SIM}, Z_{SIM}) = (X_A, Y_A, Z_A) - \begin{pmatrix} 60.336 \\ 0 \\ 0 \end{pmatrix}.$$

12.2.8 SAOSAC coordinates (HRMA-3.0)

The SAOSAC coordinate system $(X_{OSAC}, Y_{OSAC}, Z_{OSAC})$ is slightly different again. In the SAOSAC system, at XRCF, the Z-axis increases towards the SI along the FOA, while the X and Y axes are in the aperture plane with the +Y axis vertical. The origin of SAOSAC coordinates is at the CAP datum A plane, which has nodal X-coordinate $X_N(SAOSAC) = 7.378$.

$$\begin{pmatrix} X_{OSAC} \\ Y_{OSAC} \\ Z_{OSAC} \end{pmatrix} = \begin{pmatrix} Y_N \\ -Z_N \\ X_N(SAOSAC) - X_N \end{pmatrix} \tag{107}$$

12.2.9 Summary of useful HRMA Cartesian systems

$$\begin{pmatrix} X_N \\ Y_N \\ Z_N \end{pmatrix} = \begin{pmatrix} X_H - X_H(H0) \\ Y_H \\ Z_H \end{pmatrix} = \begin{pmatrix} X_N(A1) - Z_{OSAC} \\ +X_{OSAC} \\ -Y_{OSAC} \end{pmatrix} \tag{108}$$

$$= \begin{pmatrix} (SCX - SCX(H0)) * 25.4 \\ SCY * 25.4 \\ SCZ * 25.4 \end{pmatrix}$$

References

[1] TRW IF1-20, Observatory to Science Instrument ICD, 11 Jan 1996.

[2] TRW SE30, AXAF-I System Alignment Plan, D17388, 11 Jan 1996.

[3] AXAF Transmission Grating Diffraction Coordinates, ASC Memo, D.P. Huenemorder, 2 Apr 1996.

[4] EQ7-002 Rev D.

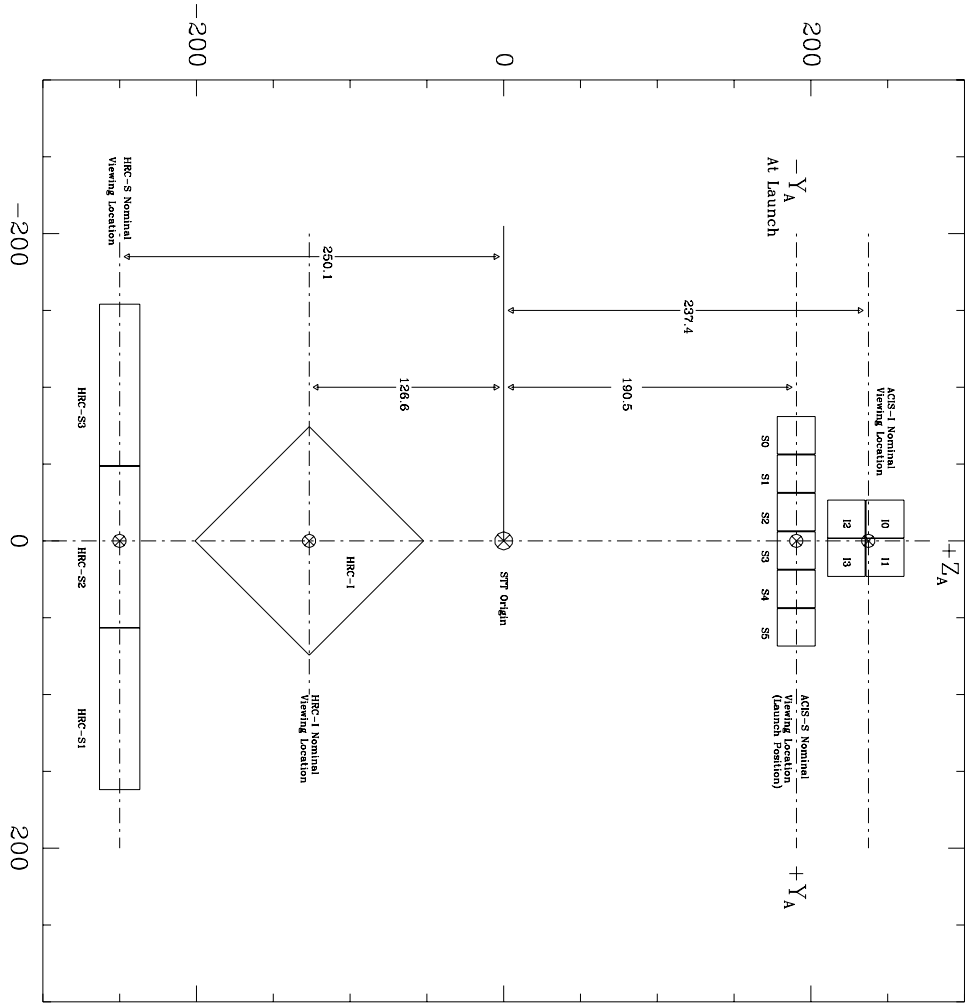

Figure 16: The AXAF SIM Translation Table, showing the flight focal plane instruments to scale. Distances are in mm. Coordinate system is AXAF-STT-1.0.

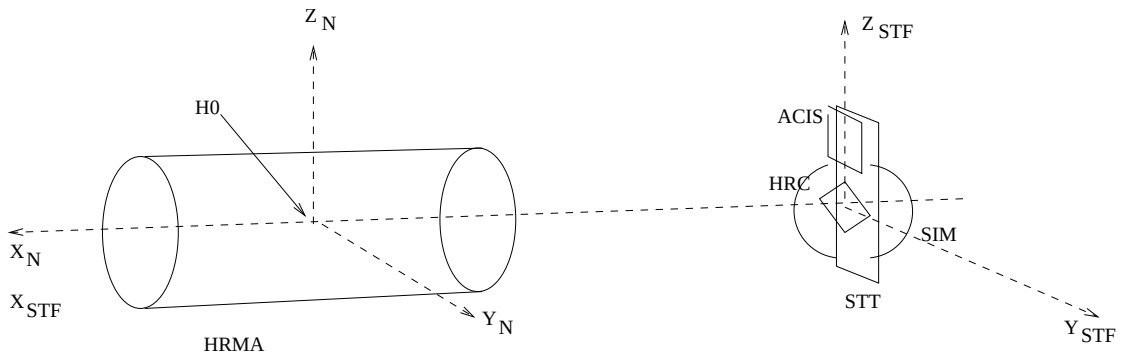

Figure 17: HRMA Nodal and STF Coordinates showing the on-orbit configuration. The SIM Transfer Table (STT) carrying the instruments moves along the Z_{STF} axis to select an instrument and along the X_{STF} axis to adjust focus.

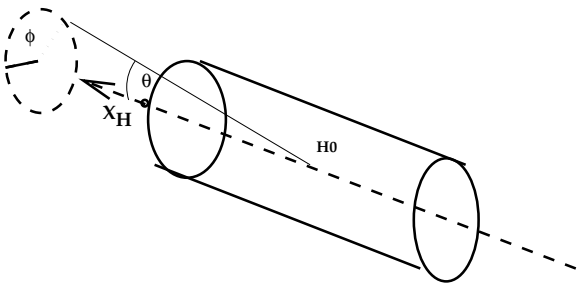

Figure 18: HRMA spherical coordinates

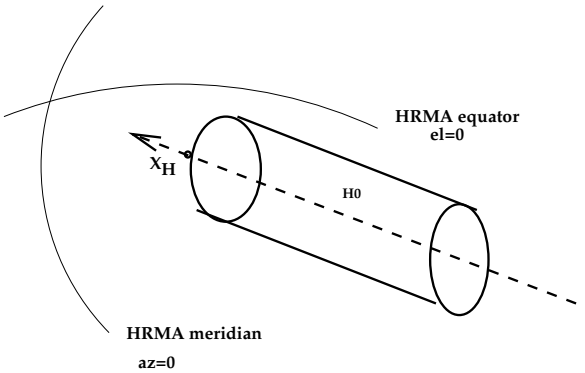

Figure 19: HRMA source coordinates

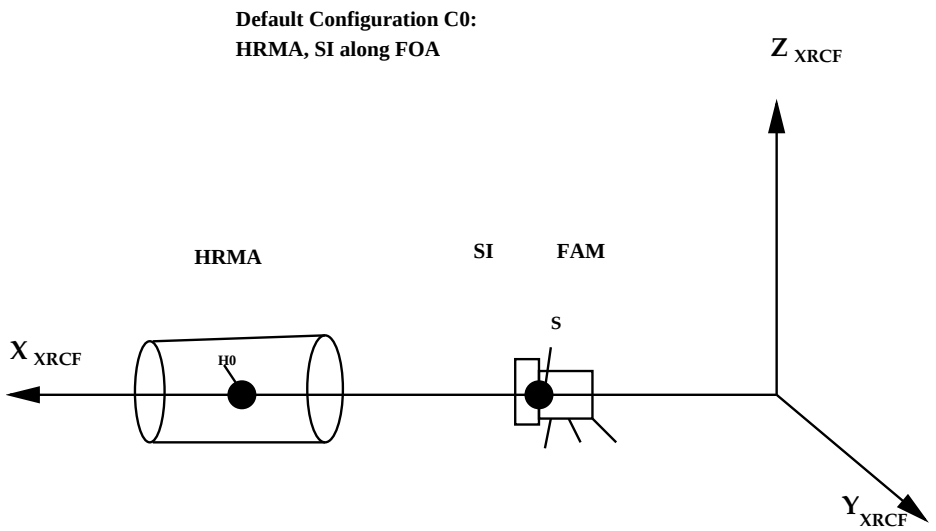

Figure 20: XRCF Coordinates showing the general configuration with HRMA, DFC and LSI coordinate systems

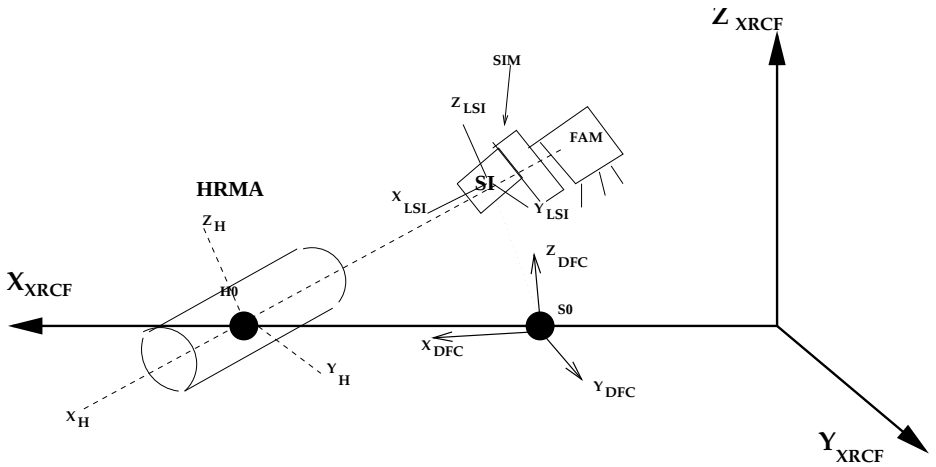

Figure 21: XRCF Coordinates showing the general configuration with HRMA and LSI coordinate systems

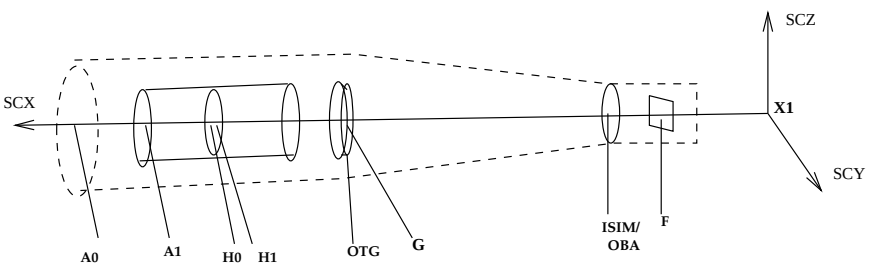

Figure 22: Schematic of interesting points in the spacecraft